Supporting Information for: Functional AdoMet isosteres resistant to classical AdoMet degradation pathways

Tyler D. Huber, Fengbin Wang, Shanteri Singh, Brooke R. Johnson, Jianjun Zhang, Manjula Sunkara, Steven G. Van Lanen, Andrew J. Morris, George N. Phillips, Jr., and Jon S. Thorson

Table of Contents

1. General materials and methods.

1.1 General materials. Unless otherwise stated, all general chemicals and reagents were purchased from Sigma-Aldrich (St. Louis, MO) or Acros (New Jersey, USA) and were reagent grade or better. *S*-adenosyl-L-methionine was purchased as a 32 mM solution in 10% EtOH/5 mM H_2SO_4 from New England Biolabs (Ipswich, MA). 7-Deazaadenosine-5′-triphosphate (^{7dz}ATP, lithium salt form) was purchased as a 100 mM solution in H_2O from TriLink Biotechnologies (San Diego, CA). *E. coli* BL21(DE3) competent cells were purchased from Invitrogen (Carlsbad, CA). The pET28a *E. coli* expression vector was purchased from Novagen (Madison, WI). Primers were purchased from Integrated DNA Technologies (Coralville, IA). Pfu DNA polymerase was purchased from Stratagene (La Jolla, CA). Restriction enzymes and T4 DNA ligase were purchased from New England Biolabs (Ipswich, MA). PD-10 columns and Ni-NTA superflow columns were purchased from GE Healthcare (Piscataway, NJ). Crystal screen kits were purchased from Hampton Research (Aliso Viejo, CA), Molecular Dimensions (Altamonte Springs, FL), Rigaku (Seattle, WA) and Microlytic (Burlington, MA).

1.2 General methods. High-throughput assay absorbance readings were conducted using a FLUOstar Omega plate reader (BMG LABTECH GmbH, Offenburg, Germany) at λ = 410 nm with a bandwidth of 2 nm and the path length was corrected to a depth corresponding to 100 µL liquid volume per well. X-ray data were collected at beamline 21-ID-F (LS-CAT) in the Advanced Photon Source at Argonne National Laboratory (Chicago, IL). NMR spectra were obtained on Varian Unity Inova 400 or 500 MHz instruments (Palo Alto, CA) at the NMR facility of the College of Pharmacy at University of Kentucky using "100%" $CDCl_3$ (D, 99.96%) with 0.05% v/v TMS, CD_3OD (D, 99.8%) with 0.05% v/v TMS, DMSO-d_6 (D, 99.9%) with or without 0.05% v/v TMS, or D_2O (D, 99.9%) from Cambridge Isotopes (Cambridge Isotope Laboratories, MA, USA). ^{1}H and ^{13}C chemical shifts were referenced to internal solvent resonances. Multiplicities are indicated by s (singlet), d (doublet), dd (doublet of doublets), t (triplet), q (quartet), quin (quintet), m (multiplet), and br (broad). Chemical shifts are reported in parts per million (ppm) and coupling constants *J* are given in Hz. Routine ^{13}C NMR spectra were fully decoupled by broad-broad WALTZ decoupling. All NMR spectra were recorded at ambient temperature.

Normal-phase flash chromatography was performed on 40–63 µm, 60 Å silica gel (Silicycle, Quebec, Canada). Analytical TLC was performed on silica gel glass TLC plates (EMD Chemical Inc). Visualization was accomplished with UV light (254 nm) followed by staining with dilute H_2SO_4 (5% in EtOH) solution, $KMnO_4$ solution (1.5 g of $KMnO_4$, 10g K_2CO_3, and 1.25 mL 10% NaOH in 200 mL water) and heating, or 10% ninhydrin in EtOH and heating. HPLC was accomplished using an Agilent 1260 system equipped with a DAD detector (Method A) or a Varian ProStar system equipped with a PDA detector (Method B). **Method A (HPLC):** To monitor the degradation of AdoMet/Ado^{t}Met/^{7dz}AdoMet/^{7dz}Ado^{t}Met and to monitor enzyme reactions, analytical reverse-phase (RP) HPLC was conducted with a Luna C_{18} (5 µm, 4.6 mm × 250 mm; Phenomenex, Torrance, California, USA) column [gradient of 1% B to 20% B over 5 min, 20% B to 55% B over 15 min, 55% B to 100% B over 1 min, 100% B for 5 min, 100% B to 1% B over 1 min, 1% B for 8 min (A = ddH_2O with 0.1% formic acid; B = acetonitrile) flow rate = 0.4 mL min^{-1}; A_{254}, A_{260}, A_{317}]. **Method B (HPLC):** To purify hMAT2A-generated ^{7dz}AdoMet and ^{7dz}Ado^{t}Met, preparative RP-HPLC was conducted with a Discovery® BIO Wide Pore C_{18} (10 µm, 21.2 × 250 mm; Supelco, Bellefonte, Pennsylvania, USA) column [gradient of 1% B to 20% B over 5 min, 20% B to 55% B over 15 min, 55% B to 100% B over 1 min, 100% B for 5 min, 100% B to 1% B over 1 min, 1% B for 8 min (A = ddH_2O with 0.1% formic acid; B = acetonitrile) flow rate = 8.0 mL min^{-1}; A_{254}]. HPLC peak areas were integrated with Star Chromatography Workstation Software (Varian, Palo Alto, CA, USA).

High resolution electrospray ionization (ESI) mass spectra (HRMS) (for L-^{t}Met) were recorded on an AB Sciex Triple TOF 5600 instrument coupled with an Eksigent Ekspert micro LC 200 system with source temperature of 150 °C, ion spray voltage floating (ISVF) of 5000 V in positive mode. Samples were infused at 20 µL min-1 and spectra collected for 3 min at a resolution greater than 31000. In negative mode ISVF of -4000 V was used. C17 lysophosphatidyl choline with a mass of 510.3554 and C17 lysophosphatidic acid with a mass of 423.2517 were used as internal references to calibrate the spectra in positive and negative modes respectively. High-resolution electrospray ionization mass spectra (for

Ado^{t}Met, ^{7dz}AdoMet, ^{7dz}Ado^{t}Met, and 2-chloro-1-methoxy-4-nitrobenzene) were recorded on a Thermo Scientific (Rockford, IL, USA) Q Exactive (Orbitrap mass spectrometer) via direct infusion at 3 µL/min. Full-scan mass spectra were recorded in positive (3.8 kV) and negative (3.8 kV) ion modes (capillary temperature: 225 °C; nominal resolution: 140,000).

Accession codes. The gene sequence of *Homo sapiens* methionine adenosyltransferase II-α (hMAT2A) and *Streptomyces peucetius* carminomycin *O*-methyltransferase (*dnrK*) involved in this study can be found at GenBank as accession numbers AAH01686.1[S1] and L40425.1,[S2] respectively. The DnrK-ClNP-AdoHcy crystal structure can be found at the Research Collaboratory for Structural Bioinformatics (RCSB) Protein Data Bank (PDB) as PDB ID 5EEH, the DnrK-Ado^{t}Hcy crystal structure can be found as PDB ID 5EEG, and the previously reported DnrK-carminomycin-AdoHcy crystal structure can be found as PDB ID 1TW2.[S3]

2. Synthesis of tetrazole-L-methionine (L-^{t}Met). The synthesis of L-^{t}Met was accomplished in four steps from commercially-available starting material. The procedures for the synthesis of L-^{t}Met described herein are derived from previously reported methods with slight modifications.[S4–S11]

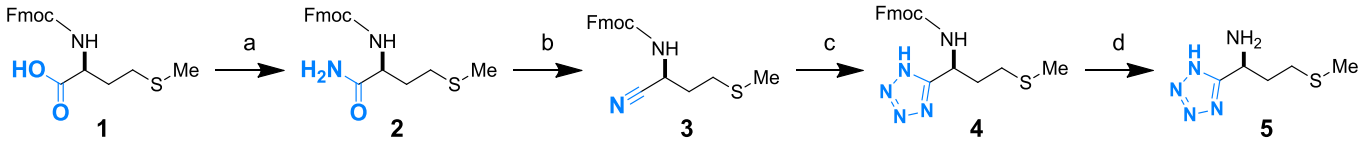

(a) $(Boc)_2O$, pyridine, NH_4HCO_3, rt, 48 h, 97%; **(b)** $(TFA)_2O$: pyridine (1:1), THF, 0°C, 3 h, 80%; **(c)** NaN_3, $ZnBr_2$, H_2O/2-propanol (2:1), 80°C, 16 h, 65%; **(d)** Et_2NH, CH_2Cl_2, 0.5 h, 82%

(*S*)-(9*H*-fluoren-9-yl)methyl [1-amino-4-(methylthio)-1-oxobutan-2-yl]carbamate (2). Fmoc-L-methionine (**1**) (10 g, 26.9 mmol) was dissolved in 300 mL of 1:1 DMF:dioxane in a round-bottom flask. To this solution was added $(Boc)_2O$ (1.1 eq., 6.5 g, 29.6 mmol), NH_4HCO_3 (1.1 eq., 2.2 g, 29.6 mmol), and pyridine (1.1 eq., 2.6 mL, 29.6 mmol). The reaction was left to stir at room temperature for 48 h under an argon atmosphere. Upon completion of the reaction, as indicated by TLC ($CHCl_3$:MeOH, 9:1), the entire reaction mixture was poured into 1.5 L of EtOAc, transferred to a separatory funnel, washed with ddH_2O (2 x 1.5 L), and 5% H_2SO_4 (1 x 1.5 L). The organic fraction was concentrated *in vacuo* to give the product as a white powder (9.7 g, 26.2 mmol, 97% yield). ^{1}H NMR (400 MHz, DMSO-d_6) δ ppm 7.85 (d, *J* = 7.5 Hz, 2 H), 7.69 (dd, *J* = 7.5, 4.0 Hz, 2 H), 7.45 (d, *J* = 8.4 Hz, 1 H), 7.38 (td, *J* = 7.5, 1.1 Hz, 2 H), 7.29 (tt, *J* = 7.4, 1.4 Hz, 2 H), 7.00 (s, 2 H), 4.31 – 4.14 (m, 3 H), 4.03 – 3.93 (m, 1 H), 2.44 – 2.32 (m, 2 H), 2.00 (s, 3 H), 1.92 – 1.69 (m, 2 H); ^{13}C NMR (100 MHz, DMSO-d_6) δ ppm 174.0, 156.4, 144.3, 144.2, 144.1 (2 carbons), 128.1 (2 carbons), 127.5 (2 carbons), 125.7 (2 carbons), 120.5 (2 carbons), 66.0, 54.1, 47.1, 32.0, 30.3, 15.0.

(*S*)-(9*H*-fluoren-9-yl)methyl [1-cyano-3-(methylthio)propyl]carbamate (3). A suspension of **2** (9.7 g, 26.2 mmol) in THF (450 mL) was stirred in a round-bottom flask at 0 °C for 15 min. After 15 min, a 1:1 solution of $(TFA)_2O$:pyridine [total volume 8.5 mL, 1.1 eq. of $(TFA)_2O$ and 2.2 eq. of pyridine] was added in drop-wise fashion via syringe and the reaction was left to stir for 3 h at 0 °C under argon. Upon completion of the reaction, as indicated by TLC ($CHCl_3$:MeOH, 9:1), 1.5 kg of crushed ice was added to the reaction mixture and the corresponding precipitated nitrile product isolated as an off-white powder via vacuum filtration. The recovered filtrate was washed with ddH_2O (500 mL) and subsequently dried via lyophilization (7.4 g, 20.9 mmol, 80% yield). ^{1}H NMR (400 MHz, DMSO-d_6) δ ppm 8.16 (d, *J* = 7.9 Hz, 1 H), 7.86 (d, *J* = 6.9 Hz, 2 H), 7.65 (d, *J* = 7.7 Hz, 2 H), 7.38 (t, *J* = 7.5 Hz, 2 H), 7.30 (t, *J* = 7.5 Hz, 2 H), 4.59 (t, *J* = 7.6 Hz, 1 H), 4.40 (d, *J* = 6.7 Hz, 2 H), 4.22 (t, *J* = 6.6 Hz, 1 H), 2.46 (m, 2 H, overlaps with DMSO-d_6), 2.01 (s, 3 H), 2.00 – 1.92 (m, 2 H); ^{13}C NMR (100 MHz, DMSO-d_6) δ ppm 155.9, 144.1 (2 carbons), 141.2 (2 carbons), 128.1 (2 carbons), 127.5 (2 carbons), 125.47 (2 carbons), 120.6 (2 carbons), 119.8, 66.3, 47.0, 41.6, 31.5, 29.2, 14.9.

(*S*)-(9*H*-fluoren-9-yl)methyl [3-(methylthio)-1-(1*H*-tetrazol-5-yl)propyl]carbamate (4). NaN_3 (2 eq., 2.7 g, 41.9 mmol) and $ZnBr_2$ (0.5 eq., 2.4 g, 10.5 mmol) was added to a stirred suspension of compound **3**

(7.4 g, 20.9 mmol) in 950 mL 2:1 ddH_2O:2-propanol in a round-bottom flask. The reaction mixture was refluxed (85 °C) with stirring for 16 h and, upon completion based upon TLC ($CHCl_3$:MeOH, 9:1), the reaction was cooled to room temperature and 3 N HCl (105 mL) and EtOAc (630 mL) were added, in respective order, with continued stirring until no solid remained. Organics were recovered via separatory funnel and the aqueous fraction was subsequently extracted with EtOAc (2 x 650 mL). The organic fractions were combined and concentrated under vacuum. The recovered crude was dissolved in 650 mL of EtOAc and recovered as the tetrazolate salt via extraction with 10% K_2CO_3 (3 x 650 mL). The combined aqueous phase was cooled to 0 °C, with stirring, and carefully acidified to pH 2.5 with 6 N HCl. The mixture was extracted with EtOAc (3 x 600 mL) and the recovered organics combined, washed with ddH_2O (1.8 L) and concentrated under vacuum to afford the desired product as an off-white powder (5.4 g, 13.6 mmol, 65% yield). ^{1}H NMR (400 MHz, DMSO-d_6) δ ppm 8.11 (d, J = 7.9 Hz, 1 H), 7.90 (d, J = 7.7 Hz, 2 H), 7.71 (t, J = 8.4 Hz, 2 H), 7.42 (t, J = 7.4 Hz, 2 H), 7.38 – 7.27 (m, 2 H), 5.06 (td, J = 8.5, 5.7 Hz, 1 H), 4.47 – 4.19 (m, 3 H), 2.50 (m, 2 H, overlaps with DMSO-d_6), 2.24 – 2.02 (m, 2 H), 2.05 (s, 3 H); ^{13}C NMR (100 MHz, DMSO-d_6) δ ppm 156.3, 144.2, 144.1 (2 carbons), 141.2 (2 carbons), 128.1 (2 carbons), 127.5 (2 carbons), 125.66, 125.63, 120.57, 120.54, 66.1, 47.1, 45.5, 32.7, 29.8, 15.0.

(*S*)-3-(methylthio)-1-(1*H*-tetrazol-5-yl)propan-1-amine (5). Compound **4** (5.4 g, 13.6 mmol) was dissolved in 300 mL DCM and treated with 100 mL Et_2NH while stirring at room temperature for 30 min. The crude reaction was concentrated under vacuum and the recovered crude, dry material was dissolved in 500 mL of H_2O and the mixture washed with 500 mL of Et_2O. The recovered aqueous phase was dried *in vacuo* to give the desired free amine as a brown-orange amorphous solid (1.9 g, 11.2 mmol, 82% yield). ^{1}H NMR (400 MHz, D_2O) δ ppm 4.93 (t, J = 6.4 Hz, 1 H), 2.48 – 2.19 (m, 4 H), 1.91 (s, 3 H); ^{13}C NMR (100 MHz, D_2O) δ ppm 158.8, 46.0, 31.4, 28.5, 13.9; HRESI calculated for $C_5H_{12}N_5S$ ([M+H]$^+$) *m*/*z* 174.0808; measured *m*/*z* 174.0804.

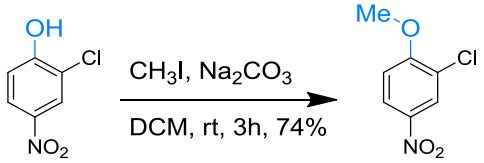

6 **7**

3. Synthesis of 2-chloro-1-methoxy-4-nitrobenzene (7). To a solution of 2-chloro-4-nitrophenol (**6**) (0.05 g, 0.29 mmol) in 5 mL DCM was added CH_3I (22 µL, 35 mmol) and Na_2CO_3 (0.03 g, 0.29 mmol) and the reaction was stirred at room temperature for 3 h. The reaction was concentrated *in vacuo*, diluted with 50 mL EtOAc, and washed with water (30 mL) and brine (30 mL). The organic phase was dried over Na_2SO_4, filtered, and the solvent was removed under reduced pressure. The residue was purified by normal phase silica gel column chromatography (using a gradient from 100:0 to 50:50, hexanes:EtOAc) to give the pure product (0.04 g, 0.21 mmol, 74% yield) as a white solid. ^{1}H NMR (400 MHz, $CDCl_3$) δ 8.27 (d, J = 2.7 Hz, 1 H), 8.15 (dd, J = 9.1, 2.7 Hz, 1 H), 6.98 (d, J = 9.1 Hz, 1 H), 4.00 (s, 3 H); ^{13}C NMR (100 MHz, $CDCl_3$) δ 160.1, 141.2, 126.0, 124.0, 123.2, 111.0, 56.8.

4. Protein crystallization, data collection, and structure refinement. Initial crystallization screens were performed using an in-house screen comprised of IndexHT, SaltHT, Peg/ion, PegRx (Hampton Research), MIDAS, Morpheus, JCSG$^+$ (Molecule Dimensions), Wizard screens 1-4 (Rigaku), and MCSG screens 1-4 (Microlytic) by the sitting drop method using a Mosquito® dispenser (TTP labTech Hertfordshire, United Kingdom). The co-crystallization crystals of DnrK and Ado^{t}Hcy were grown by mixing 0.2 µl of protein sample solution (20 mg/ml DnrK, 1 mM Ado^{t}Hcy and 20 mM Tris pH 8.0) with 0.2 µl of reservoir solution (100 mM magnesium formate dihydrate and 15% (w/v) PEG 3,350) at 20 °C using the hanging drop method. The crystals were then cryoprotected with 15% glycerol and 15% (w/v) PEG 3,350 and flash frozen in liquid nitrogen for data collection. The co-crystallization crystals of DnrK, AdoHcy and CINP were grown by mixing 0.2 µl of protein sample solution (20 mg/mL DnrK, 2.5 mM AdoMet, 7.5 mM CINP and 20 mM Tris pH 8.0) with 0.2 µL of reservoir solution (1.26 M ammonium sulfate, 0.1 M Tris pH 8.0 and 0.2 M lithium sulfate) at 20 °C using the hanging drop method. The crystals

were then soaked and cryoprotected with 80% reservoir solution, 15% glycerol and 5 mM CINP and then flash frozen in liquid nitrogen for data collection.

X-ray diffraction data were collected at the Life Sciences Collaborative Access Team (LS-CAT) with an X-ray wavelength of 0.98 Å at the Advanced Photon Source at Argonne National Laboratory. Some trail crystals were also tested at Structural Biology Center (SBC-CAT) and GM/CA at the Advanced Photon Source at Argonne National Laboratory. Data sets were indexed and scaled using HKL2000 (http://www.hkl-xray.com/how-reference-hklhkl-2000) or XDS (S12). For phasing experiments, molecular replacement was utilized using 1TW2[S3] as starting model, and then phenix.autobuild was used for automatic model building.[S13] The structural model was then completed after several rounds of manual model building with COOT[S14] and refinement with phenix.refine.[S13] Structures were visually interpreted using a stereographic collaborative commodity 3D TV arrangement.[S15] Structure quality was validated by Molprobity.[S16]

5. Supplementary references.

(S1) Strausberg, R. L., Feingold, E. a, Grouse, L. H., Derge, J. G., Klausner, R. D., Collins, F. S., Wagner, L., Shenmen, C. M., Schuler, G. D., Altschul, S. F., Zeeberg, B., Buetow, K. H., Schaefer, C. F., Bhat, N. K., Hopkins, R. F., Jordan, H., Moore, T., Max, S. I., Wang, J., Hsieh, F., Diatchenko, L., Marusina, K., Farmer, A. a, Rubin, G. M., Hong, L., Stapleton, M., Soares, M. B., Bonaldo, M. F., Casavant, T. L., Scheetz, T. E., Brownstein, M. J., Usdin, T. B., Toshiyuki, S., Carninci, P., Prange, C., Raha, S. S., Loquellano, N. a, Peters, G. J., Abramson, R. D., Mullahy, S. J., Bosak, S. a, McEwan, P. J., McKernan, K. J., Malek, J. a, Gunaratne, P. H., Richards, S., Worley, K. C., Hale, S., Garcia, A. M., Gay, L. J., Hulyk, S. W., Villalon, D. K., Muzny, D. M., Sodergren, E. J., Lu, X., Gibbs, R. a, Fahey, J., Helton, E., Ketteman, M., Madan, A., Rodrigues, S., Sanchez, A., Whiting, M., Madan, A., Young, A. C., Shevchenko, Y., Bouffard, G. G., Blakesley, R. W., Touchman, J. W., Green, E. D., Dickson, M. C., Rodriguez, A. C., Grimwood, J., Schmutz, J., Myers, R. M., Butterfield, Y. S. N., Krzywinski, M. I., Skalska, U., Smailus, D. E., Schnerch, A., Schein, J. E., Jones, S. J. M., and Marra, M. A. (2002) Generation and initial analysis of more than 15,000 full-length human and mouse cDNA sequences. *Proc. Natl. Acad. Sci. 99*, 16899–16903.

(S2) Madduri, K., Torti, F., Colombo, A. L., and Hutchinson, C. R. (1993) Cloning and sequencing of a gene encoding carminomycin 4-*O*-methyltransferase from *Streptomyces peucetius* and its expression in *Escherichia coli*. *J. Bacteriol. 175*, 3900–3904.

(S3) Jansson, A., Koskiniemi, H., Mäntsälä, P., Niemi, J., and Schneider, G. (2004) Crystal structure of a ternary complex of DnrK, a methyltransferase in daunorubicin biosynthesis, with bound products. *J. Biol. Chem. 279*, 41149–41156.

(S4) Sureshbabu, V. V., Venkataramanarao, R., Naik, S. A., and Chennakrishnareddy, G. (2007) Synthesis of tetrazole analogues of amino acids using Fmoc chemistry: isolation of amino free tetrazoles and their incorporation into peptides. *Tetrahedron Lett. 48*, 7038–7041.

(S5) Itoh, F., Yukishige, K., Wajima, M., Ootsu, K., and Akimoto, H. (1995) Non-glutamate type pyrrolo[2,3-*d*]pyrimidine antifolates. I: Synthesis and biological properties of pyrrolo[2,3-*d*]pyrimidine antifolates containing tetrazole congener of glutamic acid. *Chem. Pharm. Bull. (Tokyo). 43*, 230–235.

(S6) Pozdnev, V. F. (1995) Activation of carboxylic acids by pyrocarbonates. Application of di-*tert*-butyl pyrocarbonate as condensing reagent in the synthesis of amides of protected amino acids and peptides. *Tetrahedron Lett. 36*, 7115–7118.

(S7) Campagna, F., Carotti, A., and Casini, G. (1977) A convenient synthesis of nitriles from primary amides under mild conditions. *Tetrahedron Lett. 18*, 1813–1815.

(S8) Aureggi, V., and Sedelmeier, G. (2007) 1,3-Dipolar cycloaddition: Click chemistry for the synthesis of 5-substituted tetrazoles from organoaluminum azides and nitriles. *Angew. Chemie - Int. Ed. 46*, 8440–8444.

(S9) Demko, Z. P., and Sharpless, K. B. (2002) An expedient route to the tetrazole analogues of α-amino acids. *Org. Lett. 4*, 2525–2527.

(S10) Spero, D. M., and Kapadia, S. R. (1996) Enantioselective synthesis of α,α-disubstituted amino acid derivatives via enzymatic resolution: Preparation of a thiazolyl-substituted α-methyl α-benzyl amine. *J. Org. Chem. 61*, 7398–7401.

(S11) Demko, Z. P., and Sharpless, K. B. (2001) Preparation of 5-substituted 1*H*-tetrazoles from nitriles in water. *J. Org. Chem. 66*, 7945–50.

(S12) Kabsch, W. (2010) Xds. *Acta Crystallogr. Sect. D Biol. Crystallogr. 66*, 125–132.

(S13) Adams, P. D., Afonine, P. V., Bunkóczi, G., Chen, V. B., Davis, I. W., Echols, N., Headd, J. J., Hung, L.-W., Kapral, G. J., Grosse-Kunstleve, R. W., McCoy, A. J., Moriarty, N. W., Oeffner, R., Read, R. J., Richardson, D. C., Richardson, J. S., Terwilliger, T. C., and Zwart, P. H. (2010) PHENIX: A comprehensive Python-based system for macromolecular structure solution. *Acta Crystallogr. D. Biol. Crystallogr. 66*, 213–21.

(S14) Emsley, P., and Cowtan, K. (2004) Coot: model-building tools for molecular graphics. *Acta Crystallogr. D. Biol. Crystallogr. 60*, 2126–32.

(S15) Yennamalli, R., Arangarasan, R., Bryden, A., Gleicher, M., and Phillips, G. N. (2014) Using a commodity high-definition television for collaborative structural biology. *J. Appl. Crystallogr. 47*, 1153–1157.

(S16) Chen, V. B., Arendall, W. B., Headd, J. J., Keedy, D. a., Immormino, R. M., Kapral, G. J., Murray, L. W., Richardson, J. S., and Richardson, D. C. (2010) MolProbity: All-atom structure validation for macromolecular crystallography. *Acta Crystallogr. Sect. D Biol. Crystallogr. 66*, 12–21.

6. NMR and MS characterization.

(*S*)-(9*H*-fluoren-9-yl)methyl [1-amino-4-(methylthio)-1-oxobutan-2-yl]carbamate (**2**): ^{1}H NMR (400 MHz, DMSO-d_6)

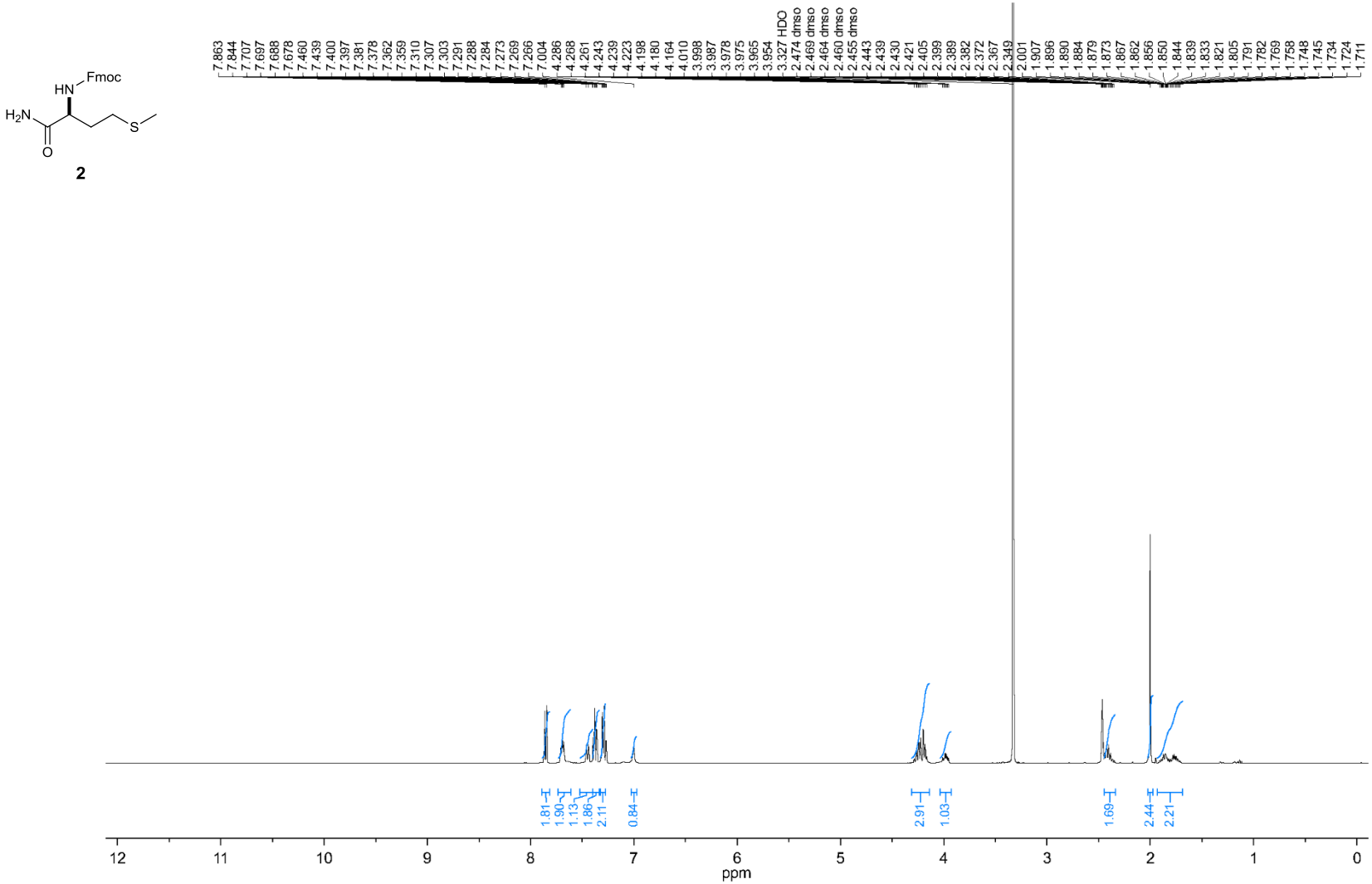

(*S*)-(9*H*-fluoren-9-yl)methyl [1-cyano-3-(methylthio)propyl]carbamate (**3**): ^{1}H NMR (400 MHz, DMSO-d_6)

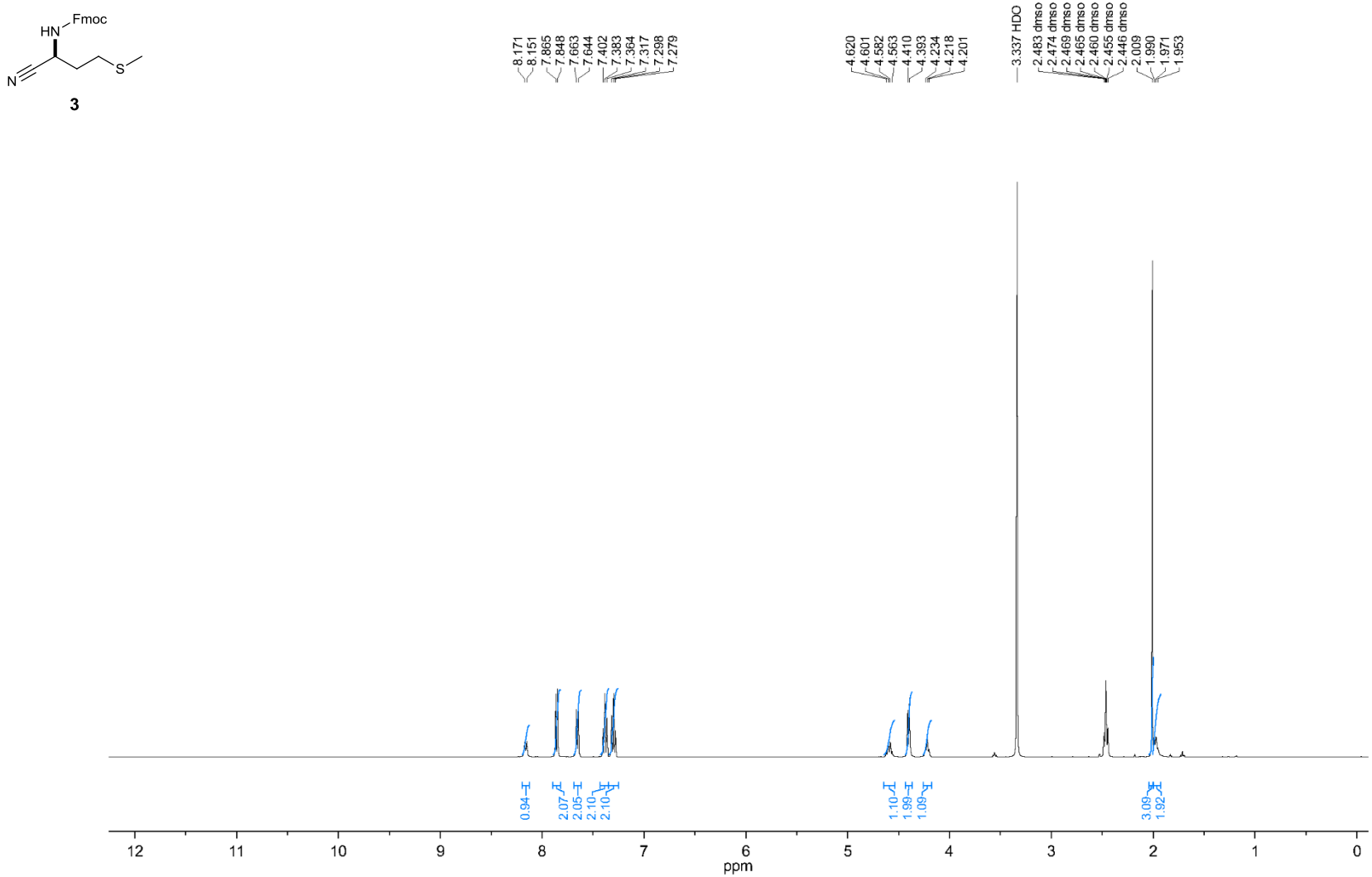

(*S*)-(9*H*-fluoren-9-yl)methyl [3-(methylthio)-1-(1*H*-tetrazol-5-yl)propyl]carbamate (**4**): ^{1}H NMR (400 MHz, DMSO-d_6)

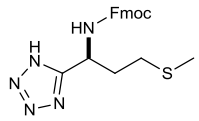

4

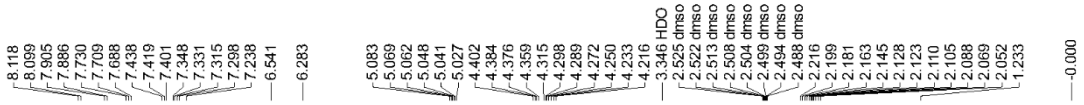

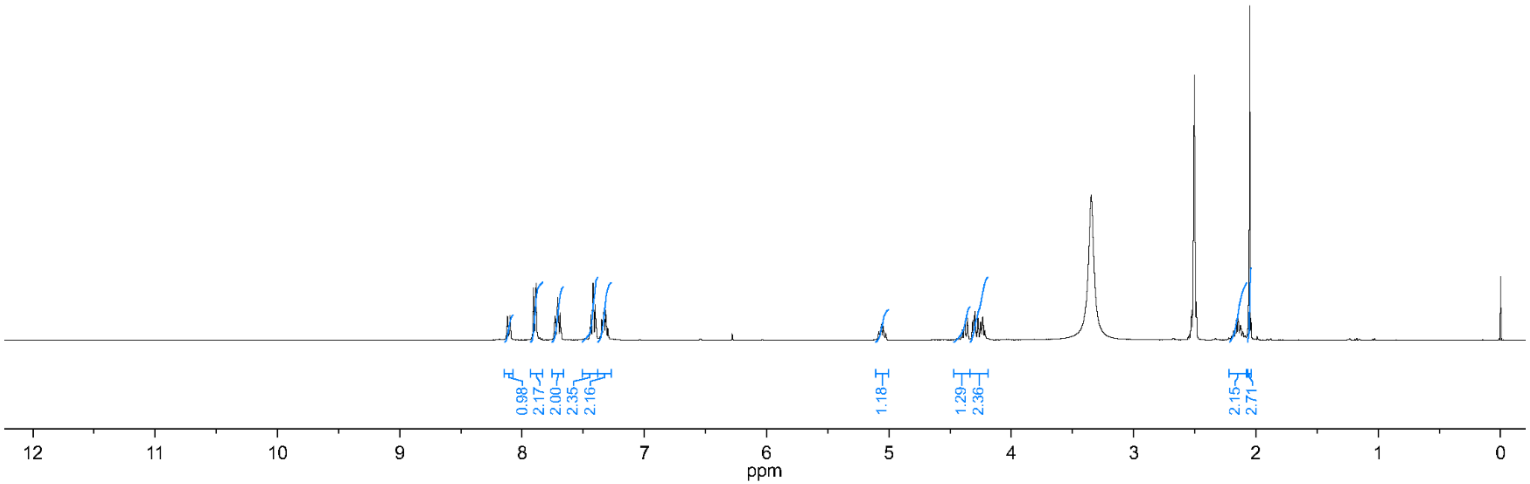

(*S*)-3-(methylthio)-1-(1*H*-tetrazol-5-yl)propan-1-amine (**5**): ^{1}H NMR (400 MHz, D_2O)

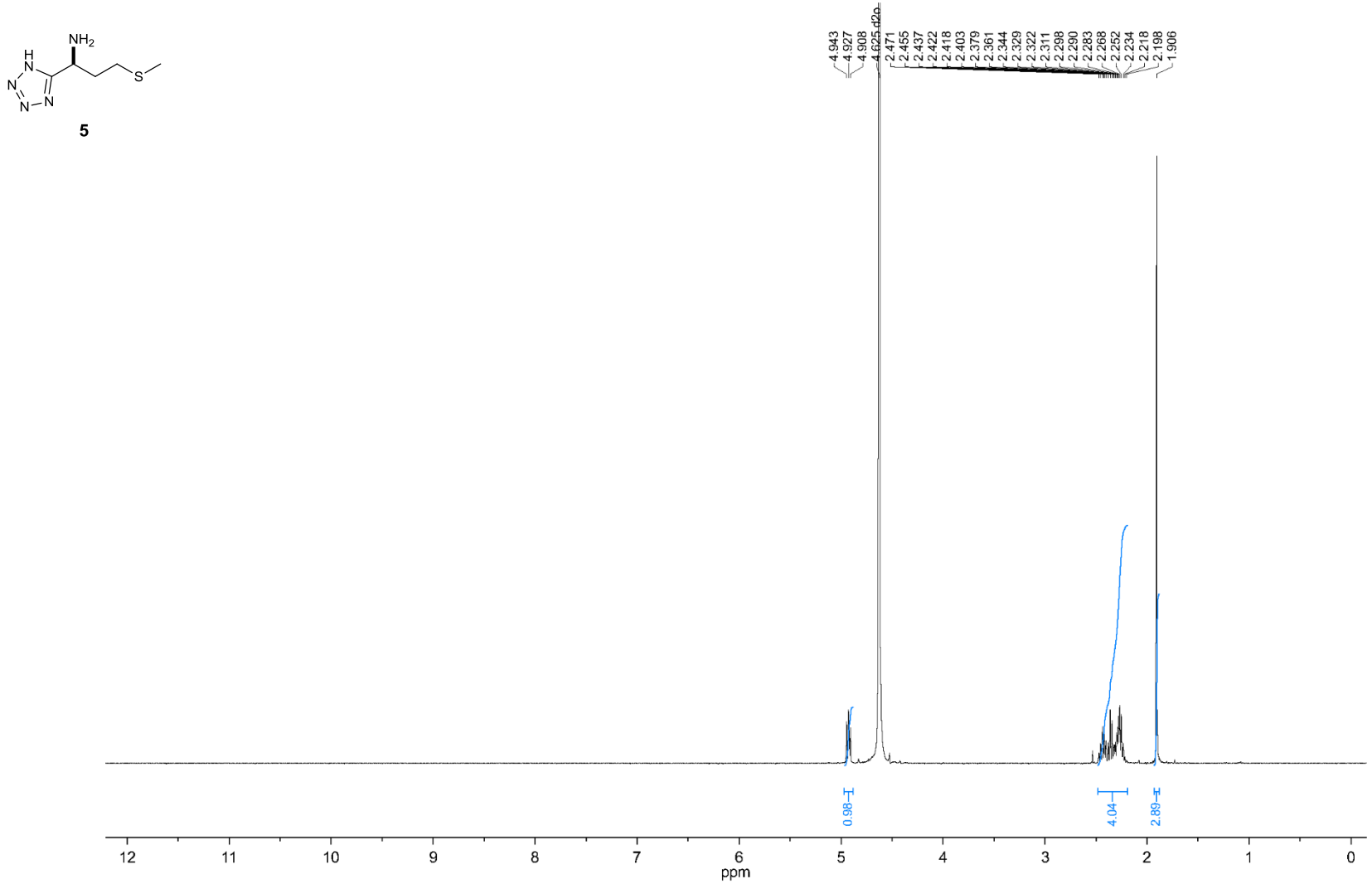

(*S*)-(9*H*-fluoren-9-yl)methyl [1-amino-4-(methylthio)-1-oxobutan-2-yl]carbamate (**2**): ^{13}C NMR (100 MHz, DMSO-d_6)

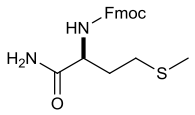

2

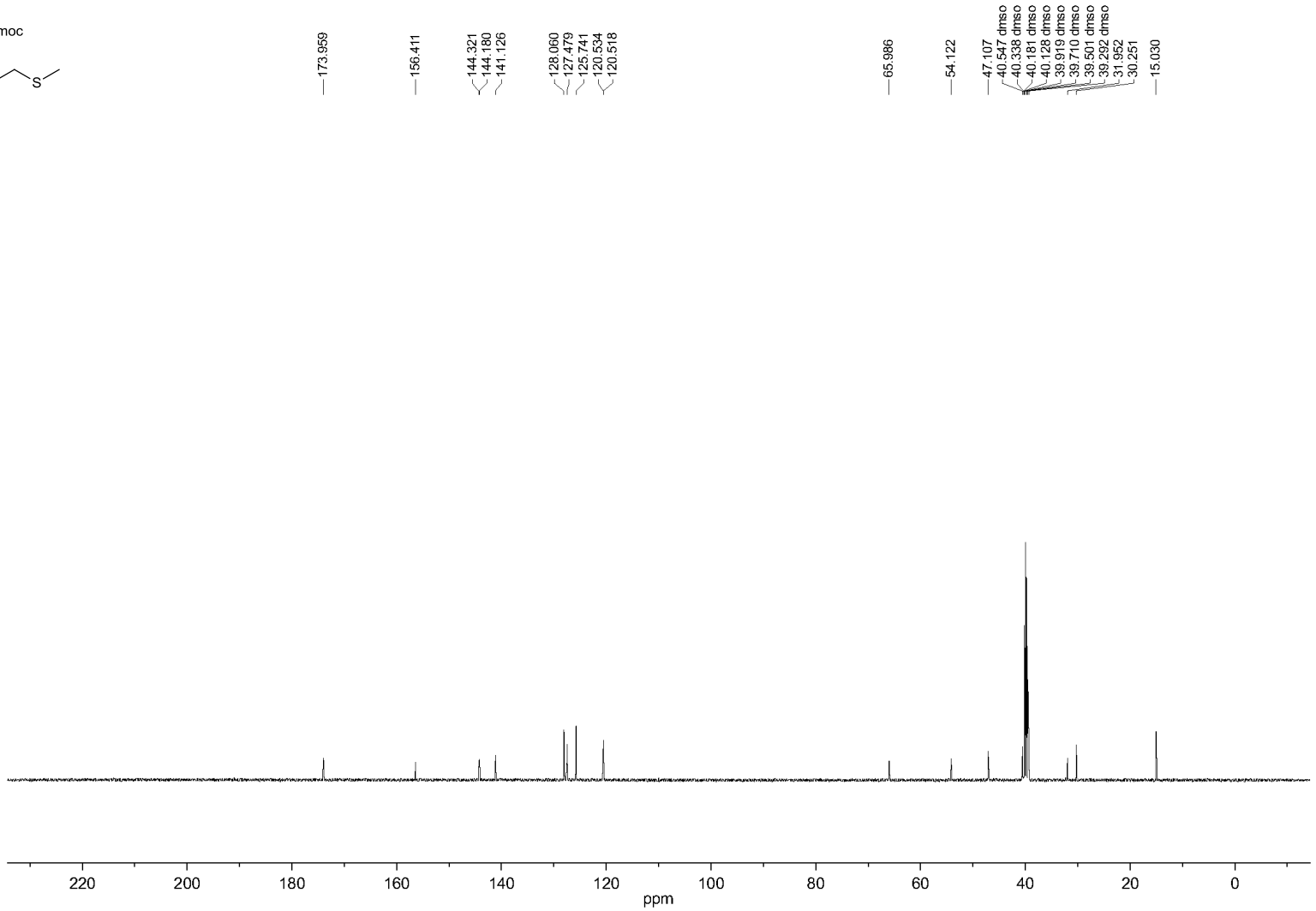

(*S*)-(9*H*-fluoren-9-yl)methyl [1-cyano-3-(methylthio)propyl]carbamate (**3**): ^{13}C NMR (100 MHz, DMSO-d_6)

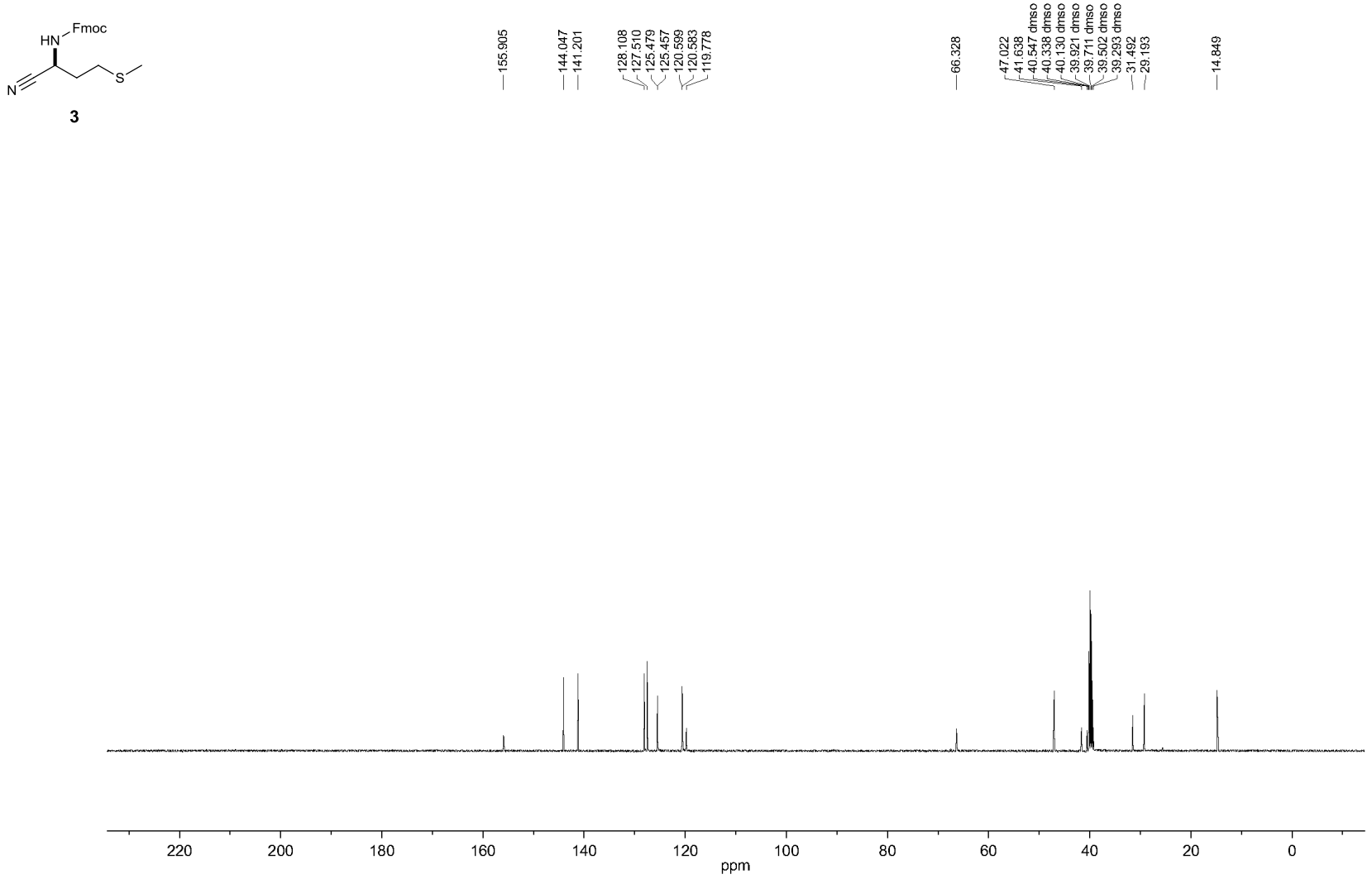

(*S*)-(9*H*-fluoren-9-yl)methyl [3-(methylthio)-1-(1*H*-tetrazol-5-yl)propyl]carbamate (**4**): ^{13}C NMR (100 MHz, DMSO-d_6)

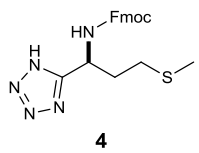

4

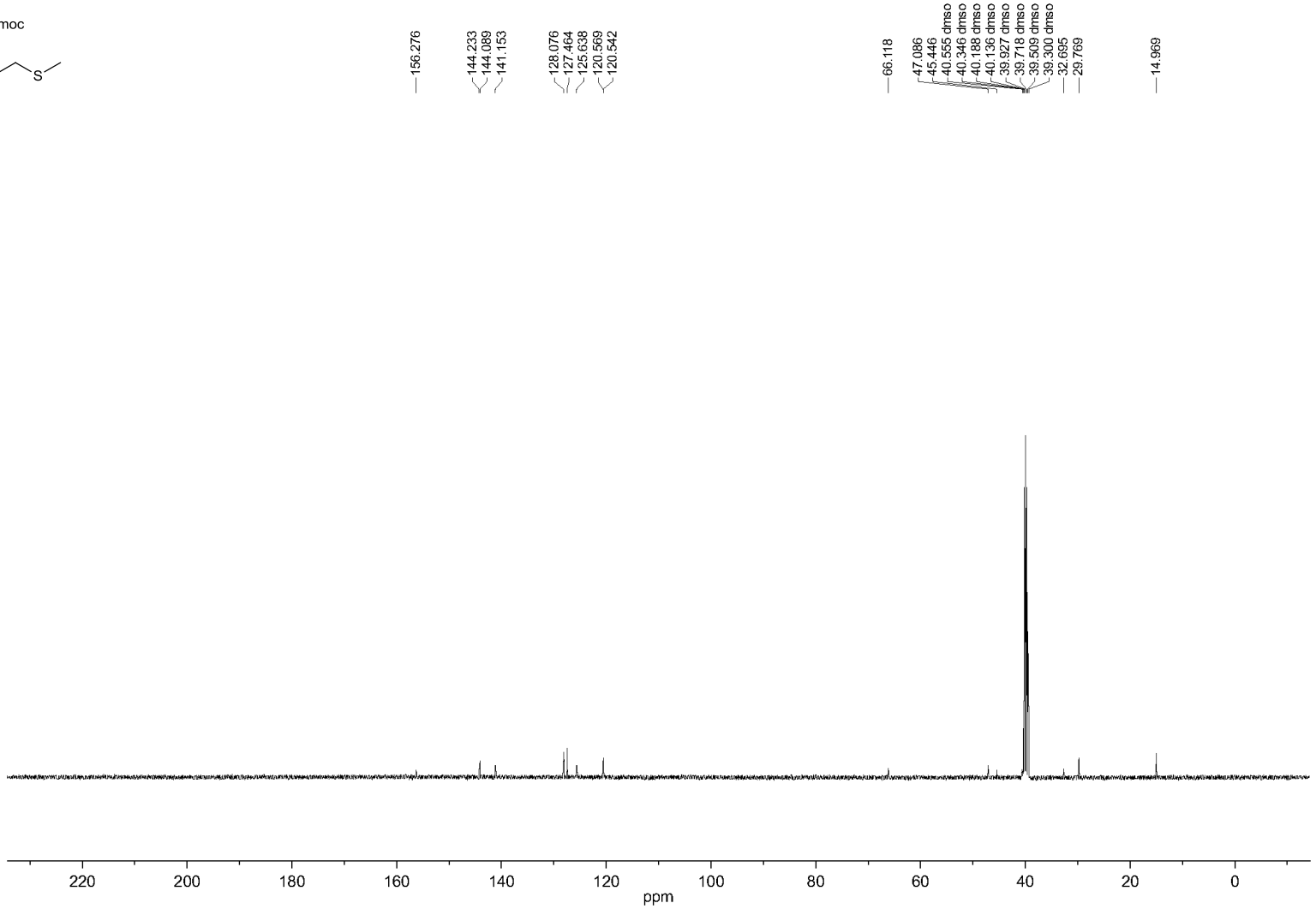

(*S*)-3-(methylthio)-1-(1*H*-tetrazol-5-yl)propan-1-amine (**5**): ^{13}C NMR (100 MHz, D_2O)

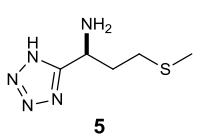

5

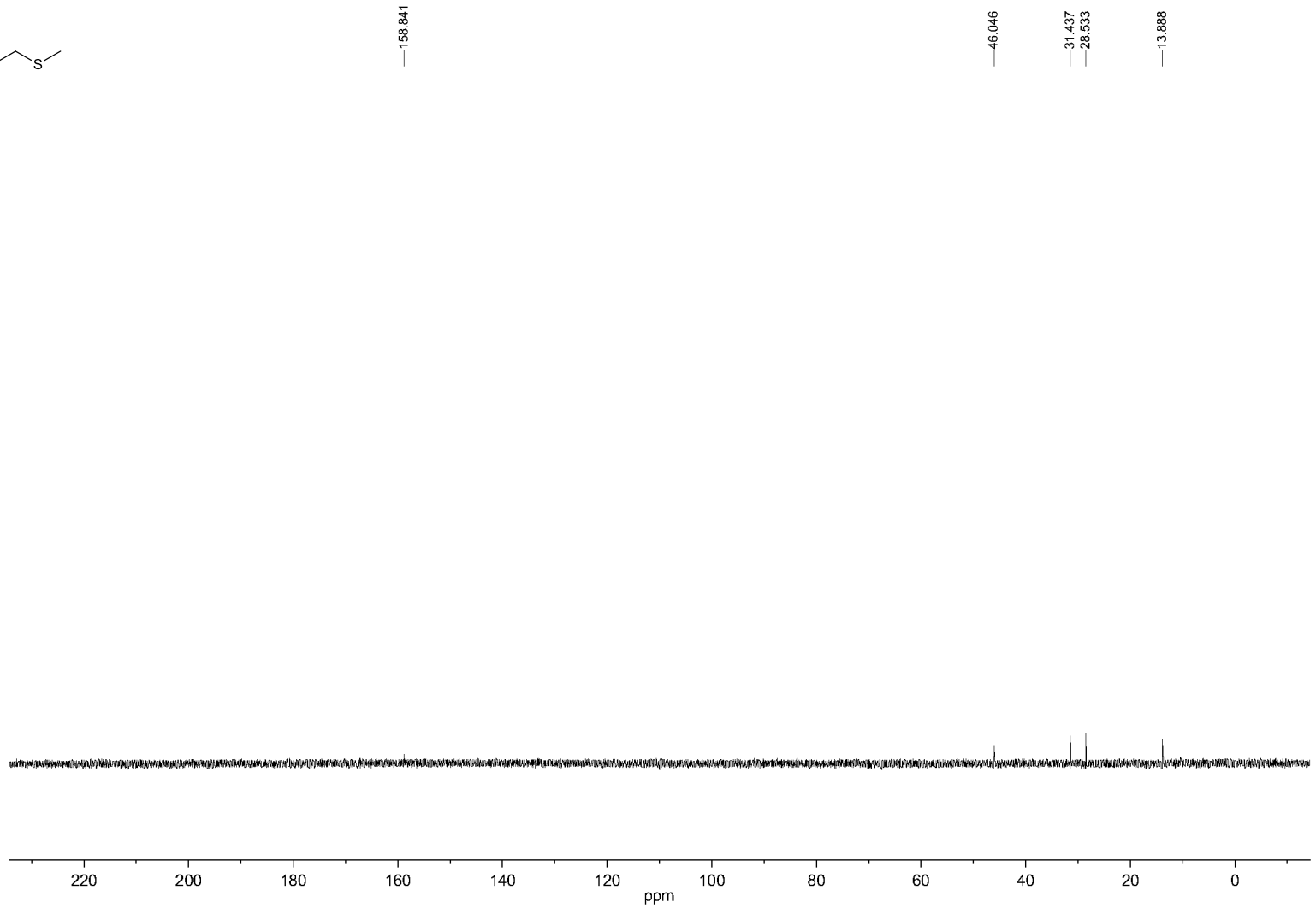

2-chloro-1-methoxy-4-nitrobenzene (**7**): ^{1}H NMR (400 MHz, $CDCl_3$)

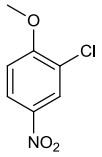

7

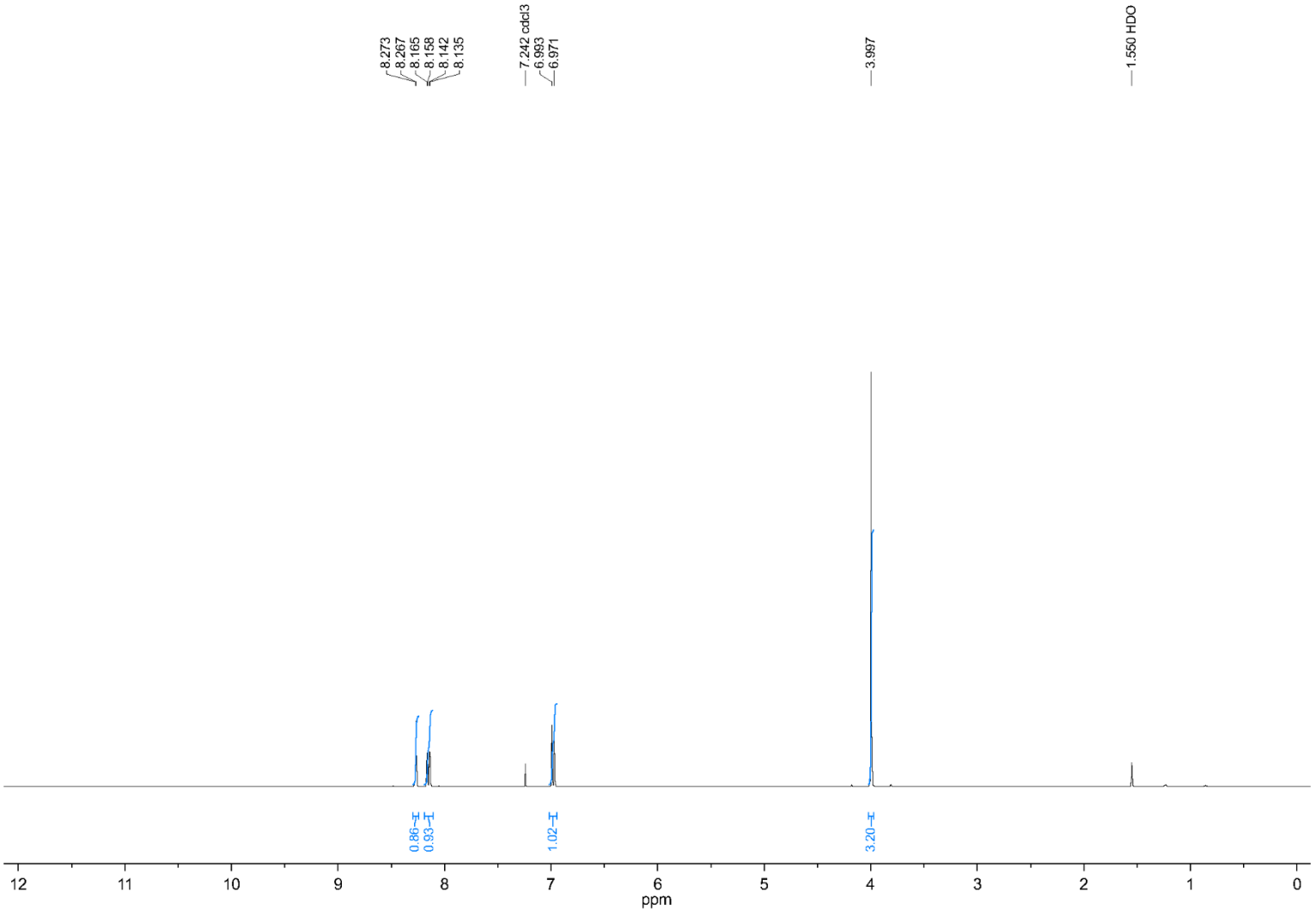

2-chloro-1-methoxy-4-nitrobenzene (**7**): ^{13}C NMR (100 MHz, $CDCl_3$)

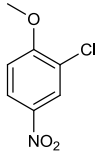

7

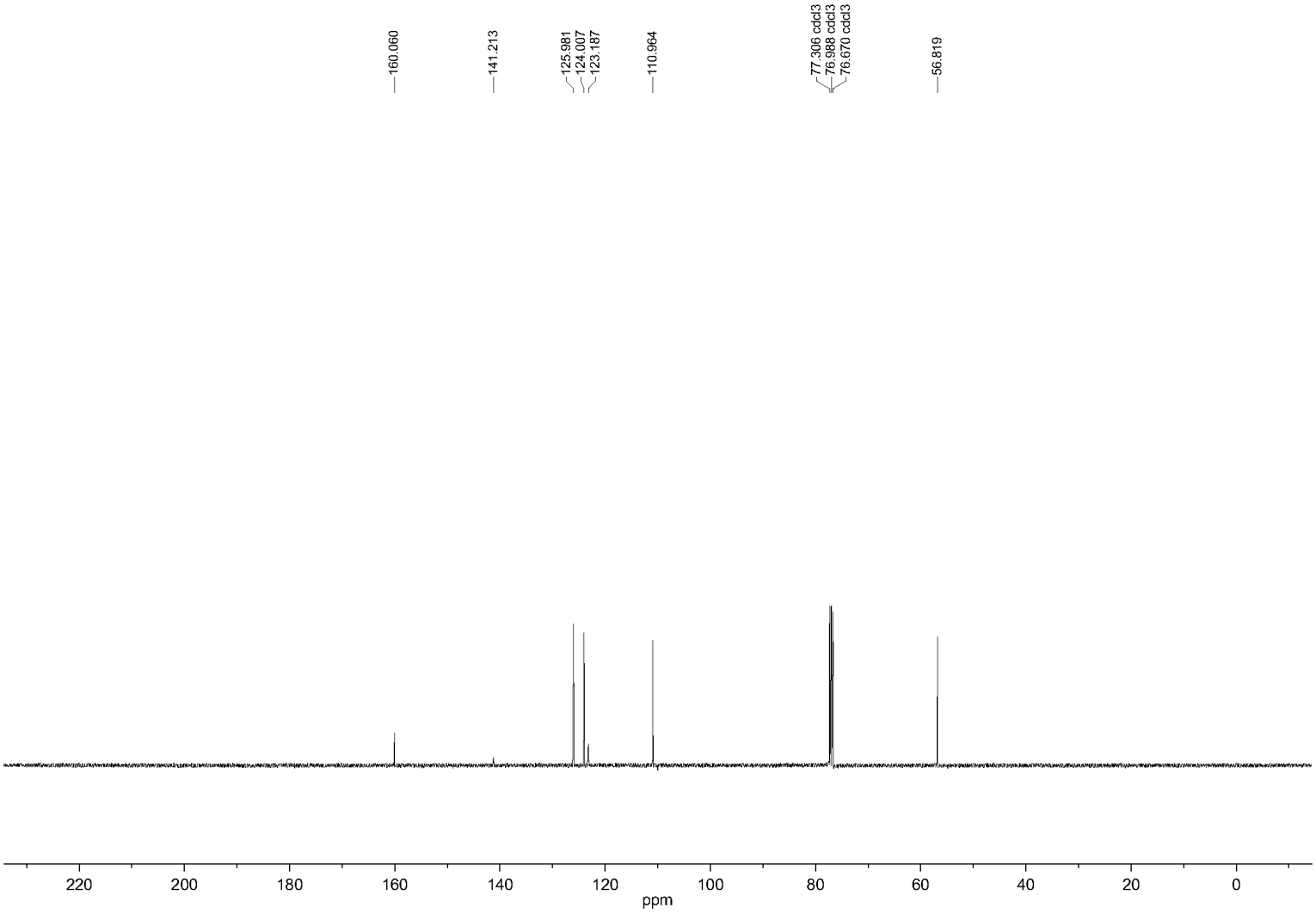

2-chloro-1-methoxy-4-nitrobenzene (**7**): gCOSY NMR (400 MHz, $CDCl_3$)

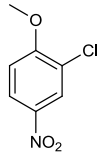

7

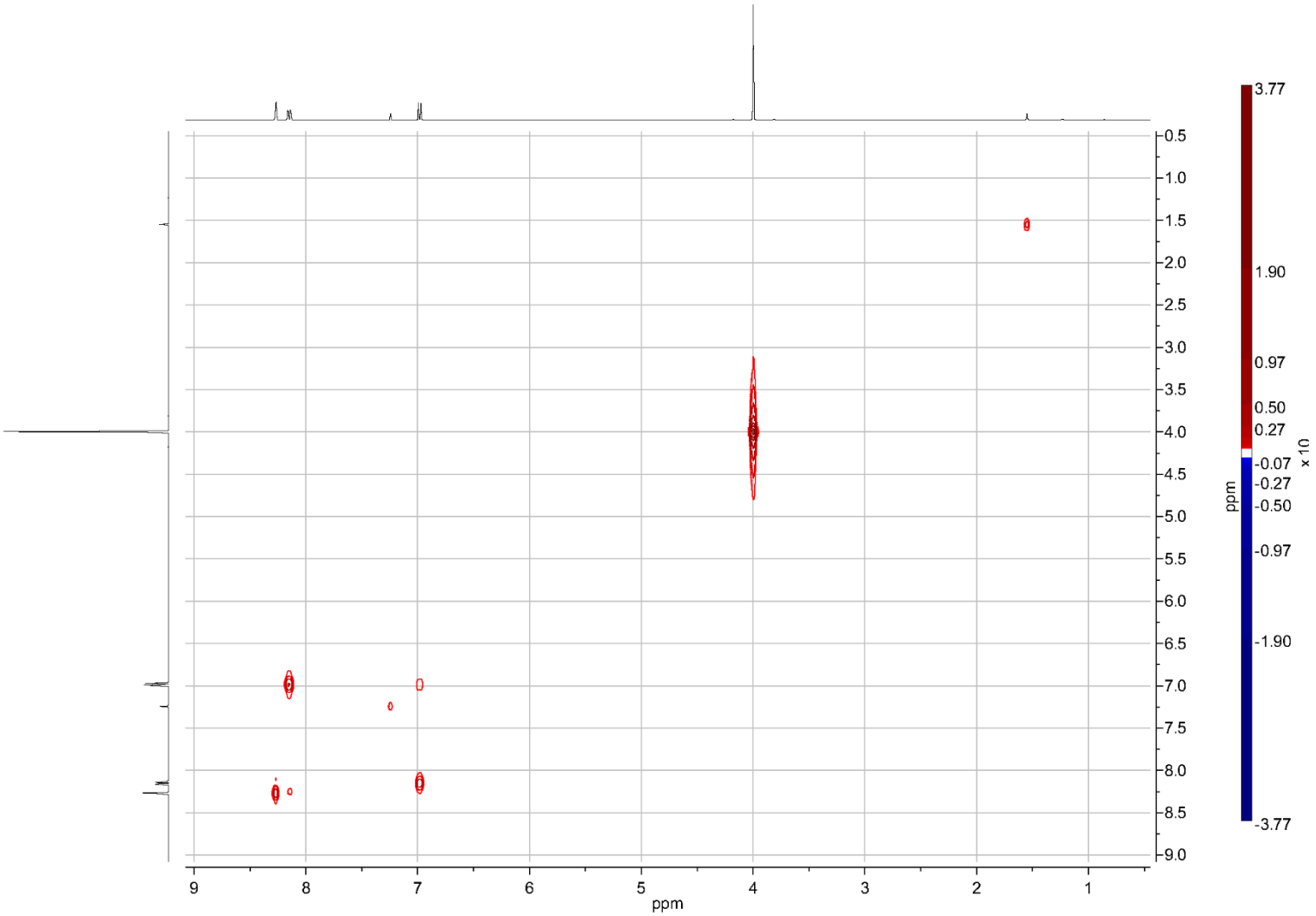

(*S*)-[(*S*)-3-amino-3-(1*H*-tetrazol-5-yl)propyl](5-adenosyl)(methyl)sulfonium (**8**): ^{1}H NMR (500 MHz, DMSO-d_6) δ ppm 8.37 (s, 1 H), 8.17 (s, 1 H), 7.34 (s, 2 H), 5.94 (d, *J* = 5.3 Hz, 1 H), 4.79 – 4.75 (m, 1 H), 4.35 – 4.29 (m, 2H), 4.10 (t, *J* = 5.5 Hz, 1 H), 4.00 – 3.92 (m, 1 H), 3.71 (d, *J* = 12.1 Hz, 1 H), 3.41 (t, *J* = 6.9 Hz, 2 H), 2.85 (s, 3 H), 2.19 – 2.04 (m, 2 H).

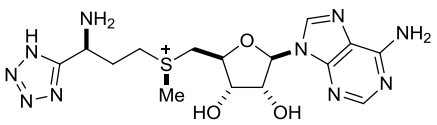

Ado^{t}Met (**8**)

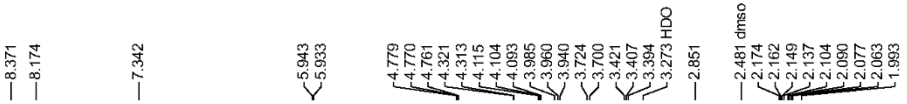

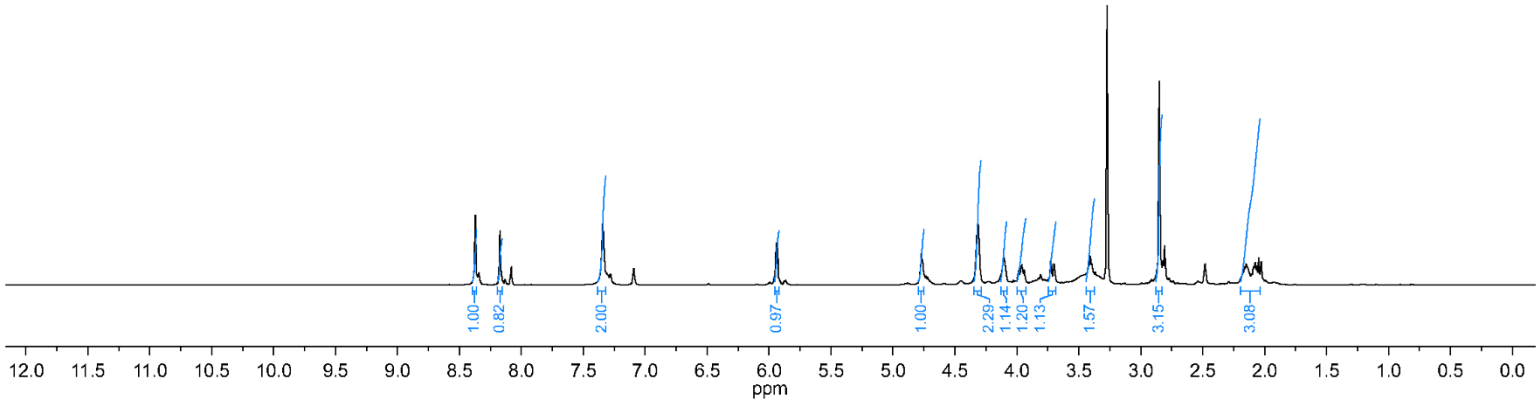

(*S*)-[(*S*)-3-amino-3-(1*H*-tetrazol-5-yl)propyl](5-adenosyl)(methyl)sulfonium (**8**): gCOSY (^{1}H-^{1}H) NMR (500 MHz, DMSO-d_6)

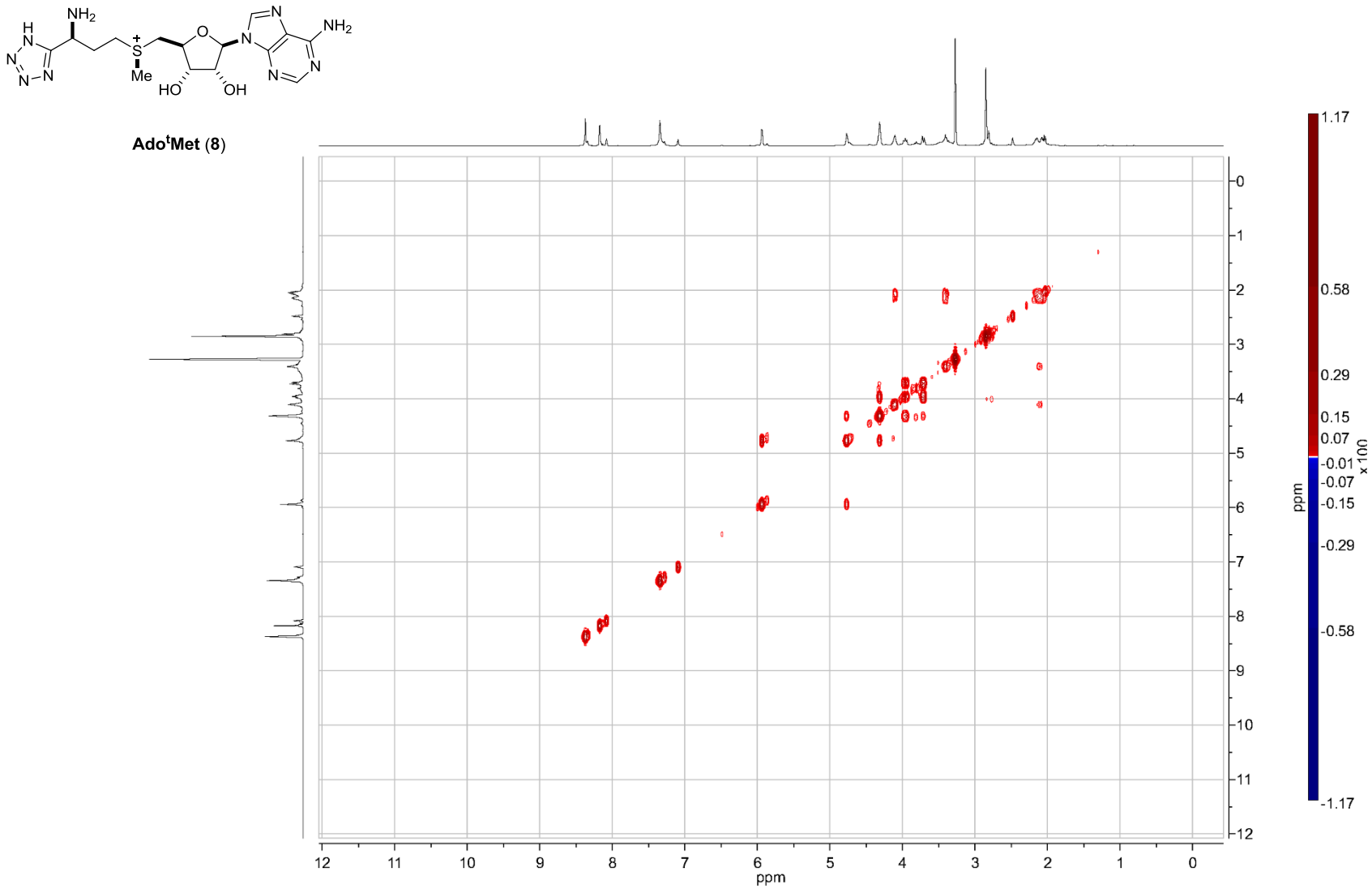

(*S*)-[(*S*)-3-amino-3-(1*H*-tetrazol-5-yl)propyl](5-adenosyl)(methyl)sulfonium (**8**): TOCSY NMR (500 MHz, DMSO-d_6)

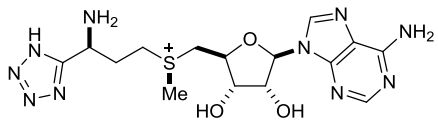

Ado^{t}Met (8)

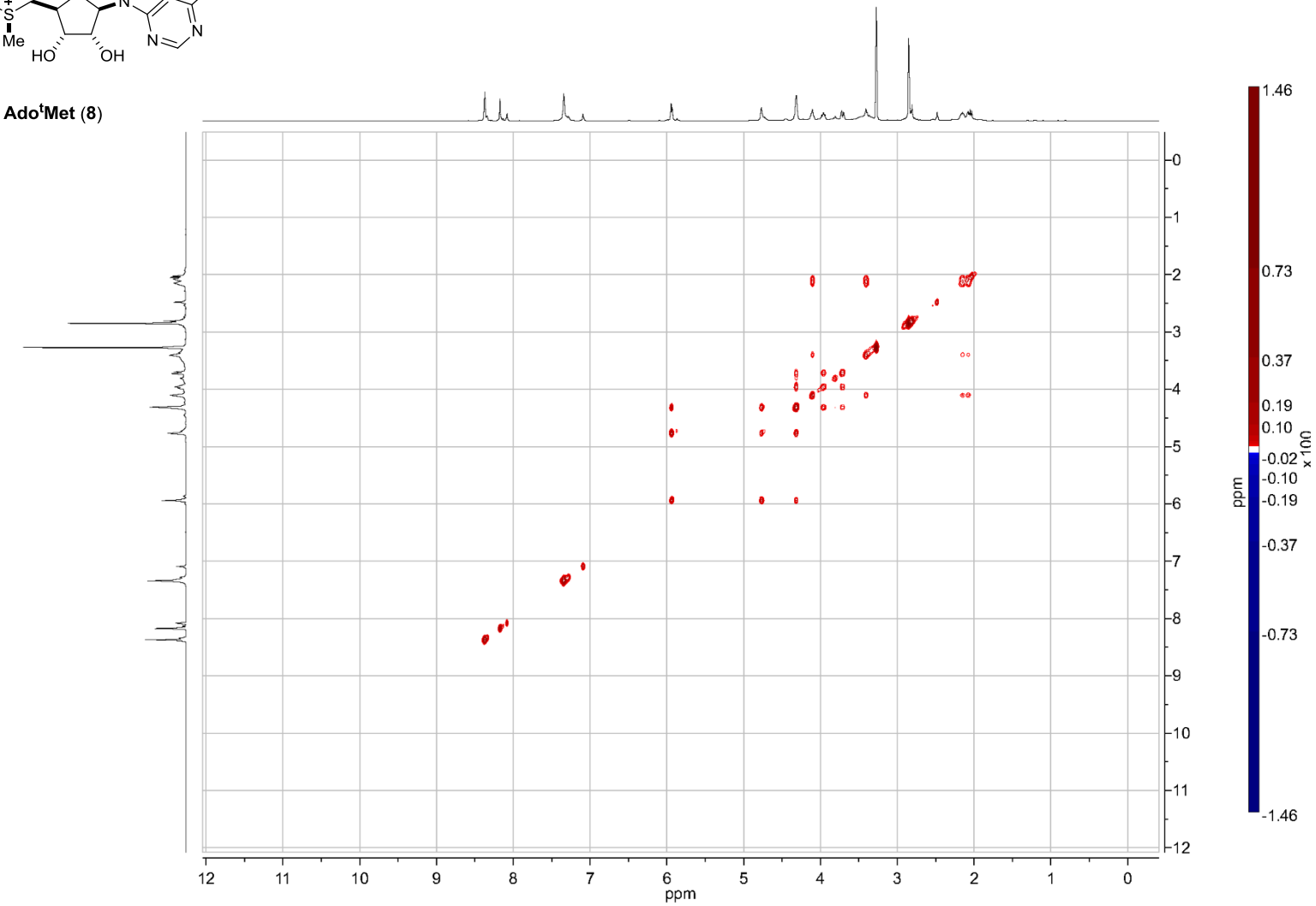

(*S*)-[(*S*)-3-amino-3-(1*H*-tetrazol-5-yl)propyl](5-adenosyl)(methyl)sulfonium (**8**): NOESY NMR (500 MHz, DMSO-d_6)

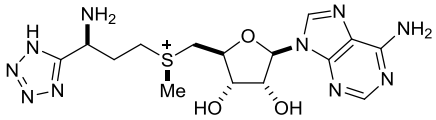

Ado^{t}Met (8)

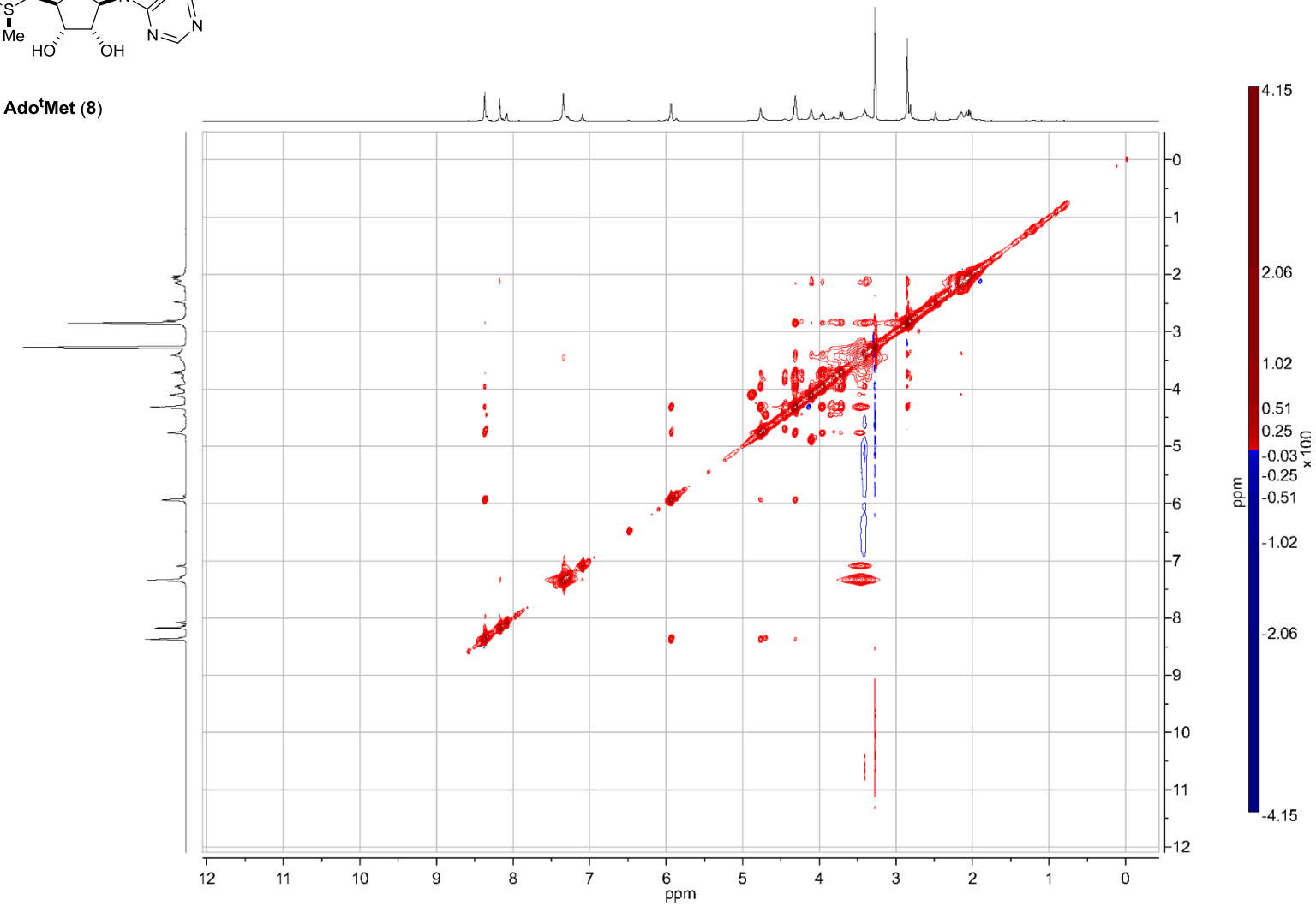

(*S*)-[(*S*)-3-amino-3-(1*H*-tetrazol-5-yl)propyl](5-adenosyl)(methyl)sulfonium (**8**): gHSQC NMR (500 MHz, DMSO-d_6)

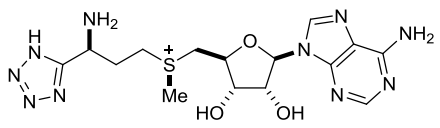

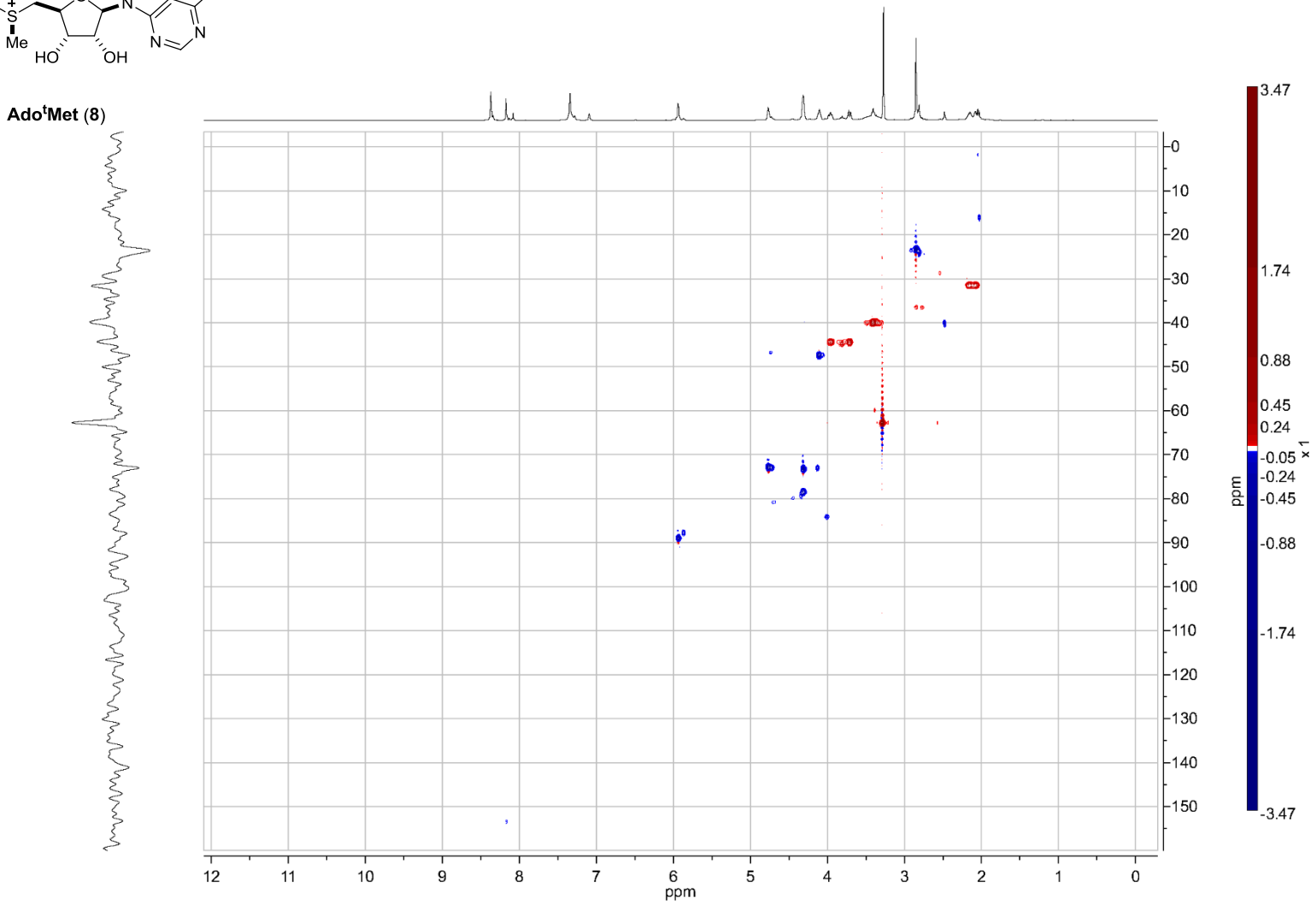

(*S*)-[(*S*)-3-amino-3-(1*H*-tetrazol-5-yl)propyl](5-adenosyl)(methyl)sulfonium (**8**): gHMBC NMR (500 MHz, DMSO-d_6)

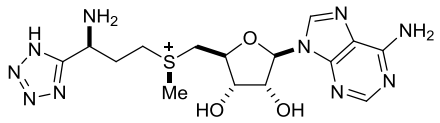

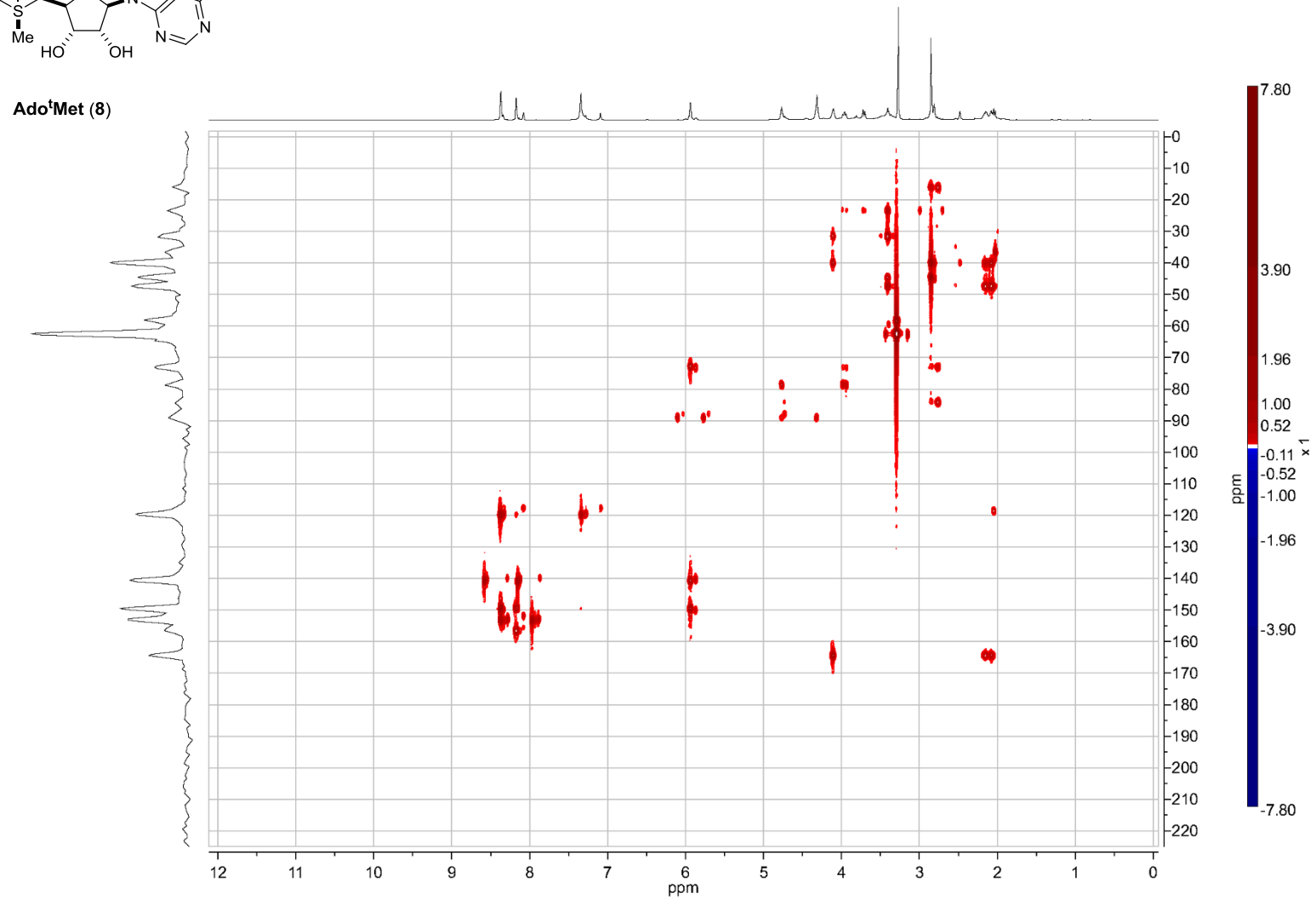

HRMS of tMet (**5**)

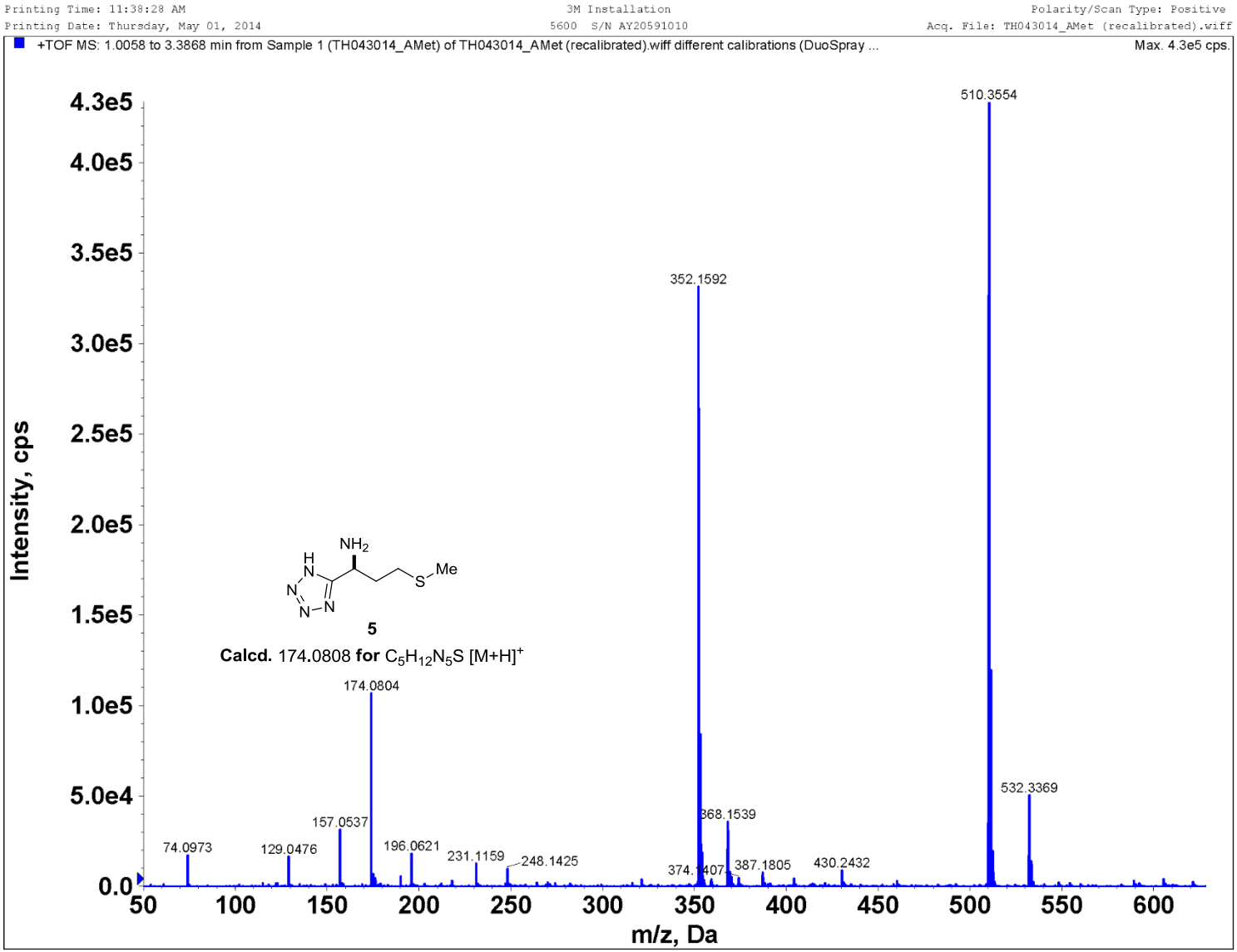

HRMS of Ado^{t}Met (**8**)

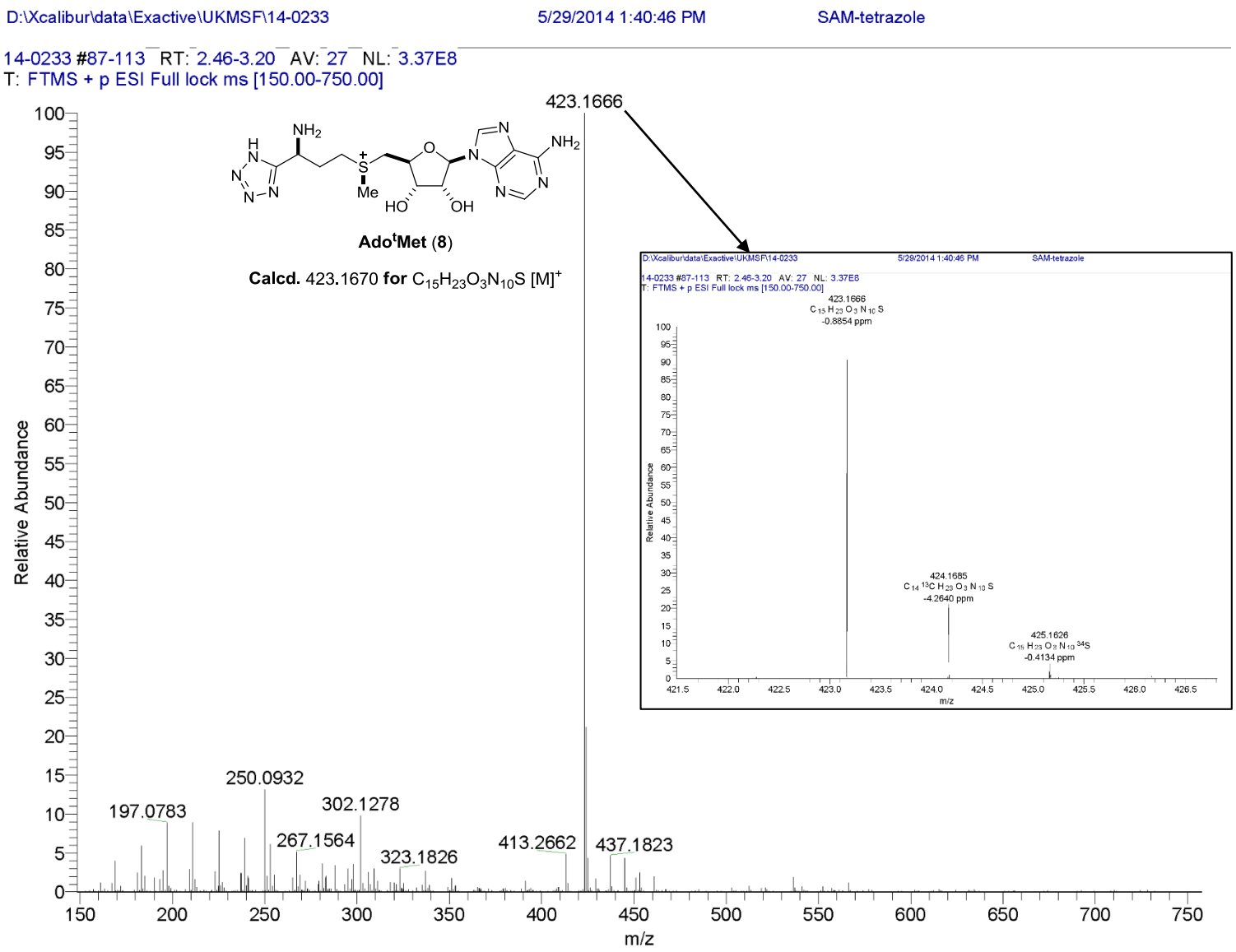

HRMS of ^{7dz}AdoMet (**9**)

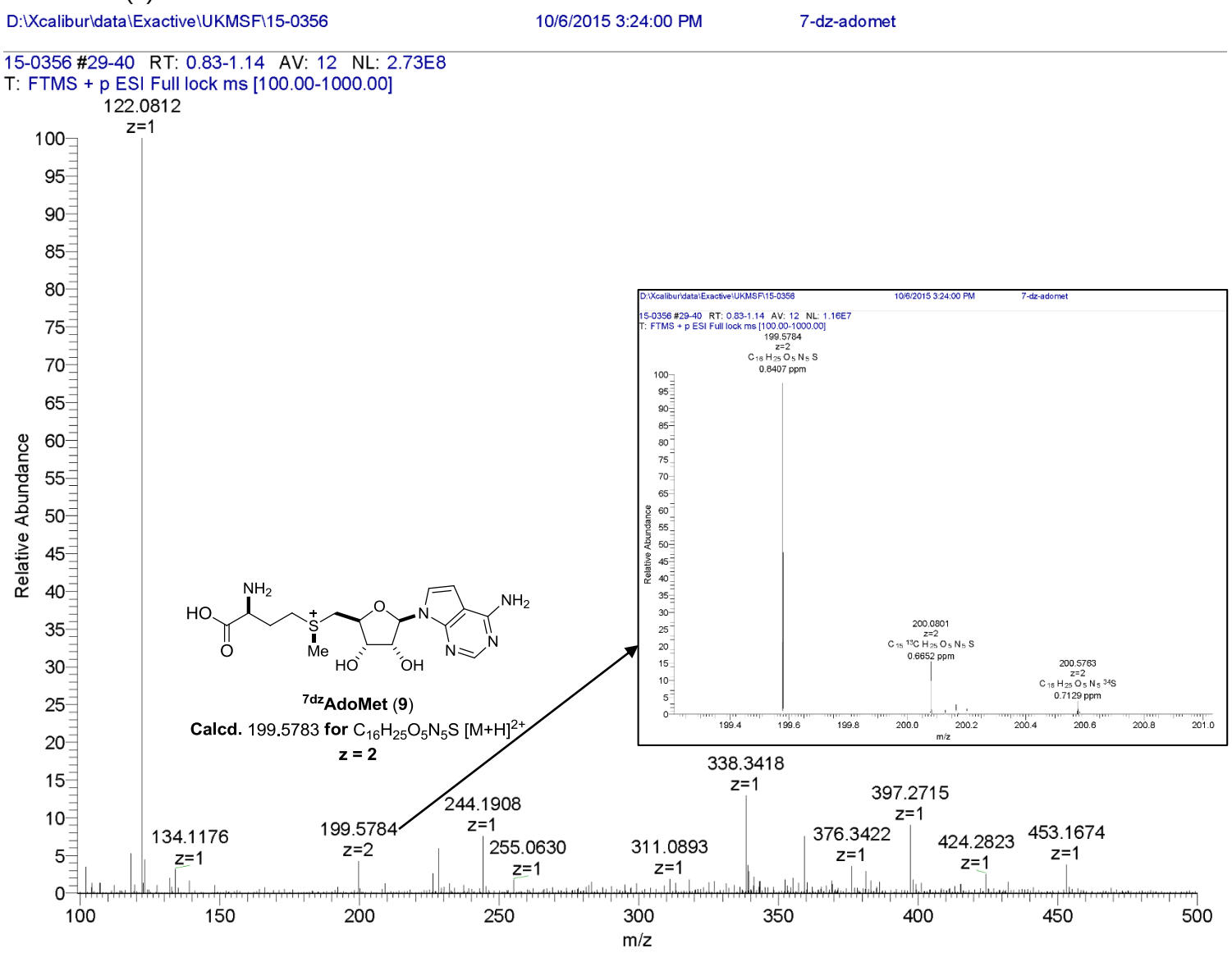

HRMS of ^{7dz}Ado^{t}Met (**10**)

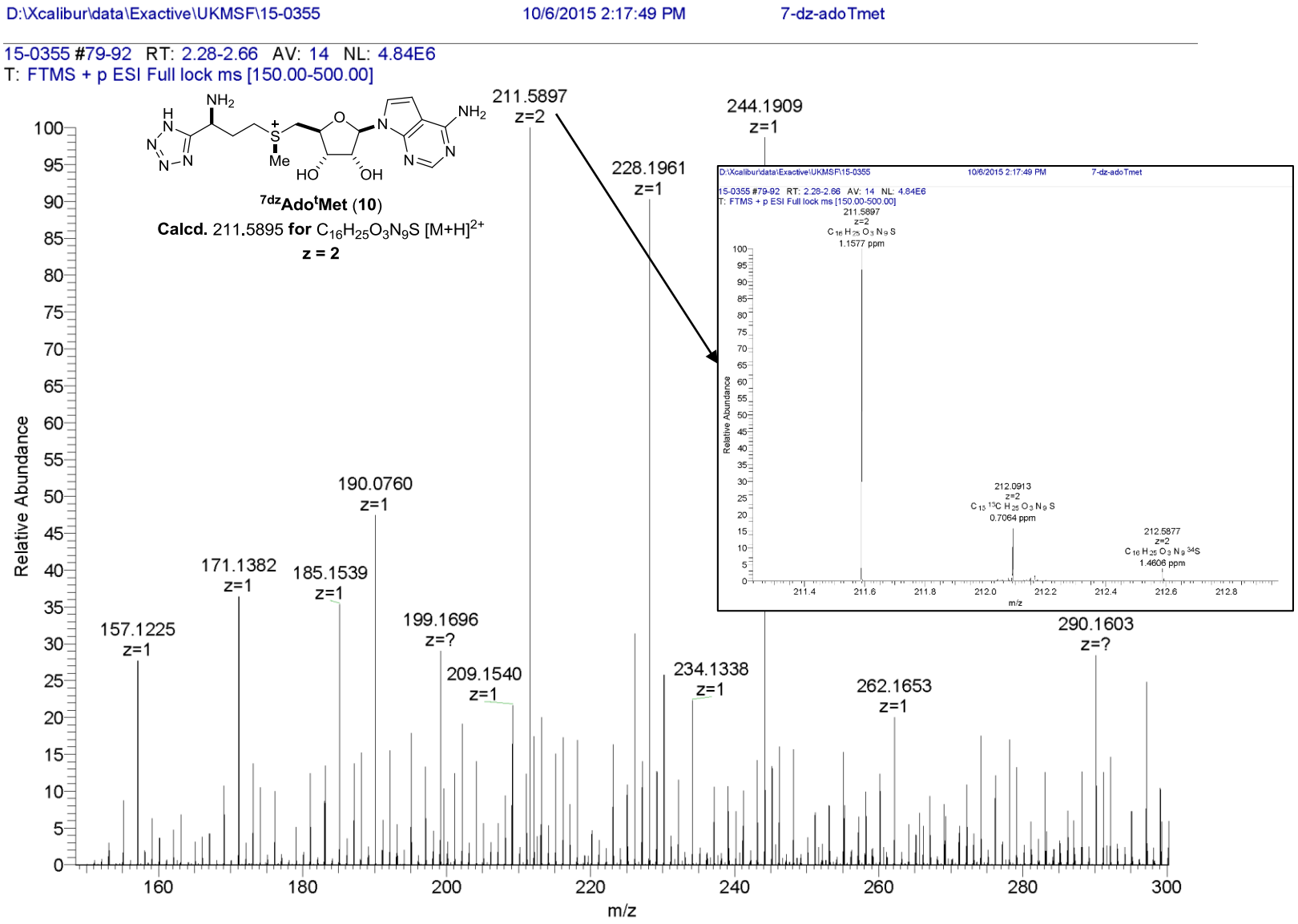

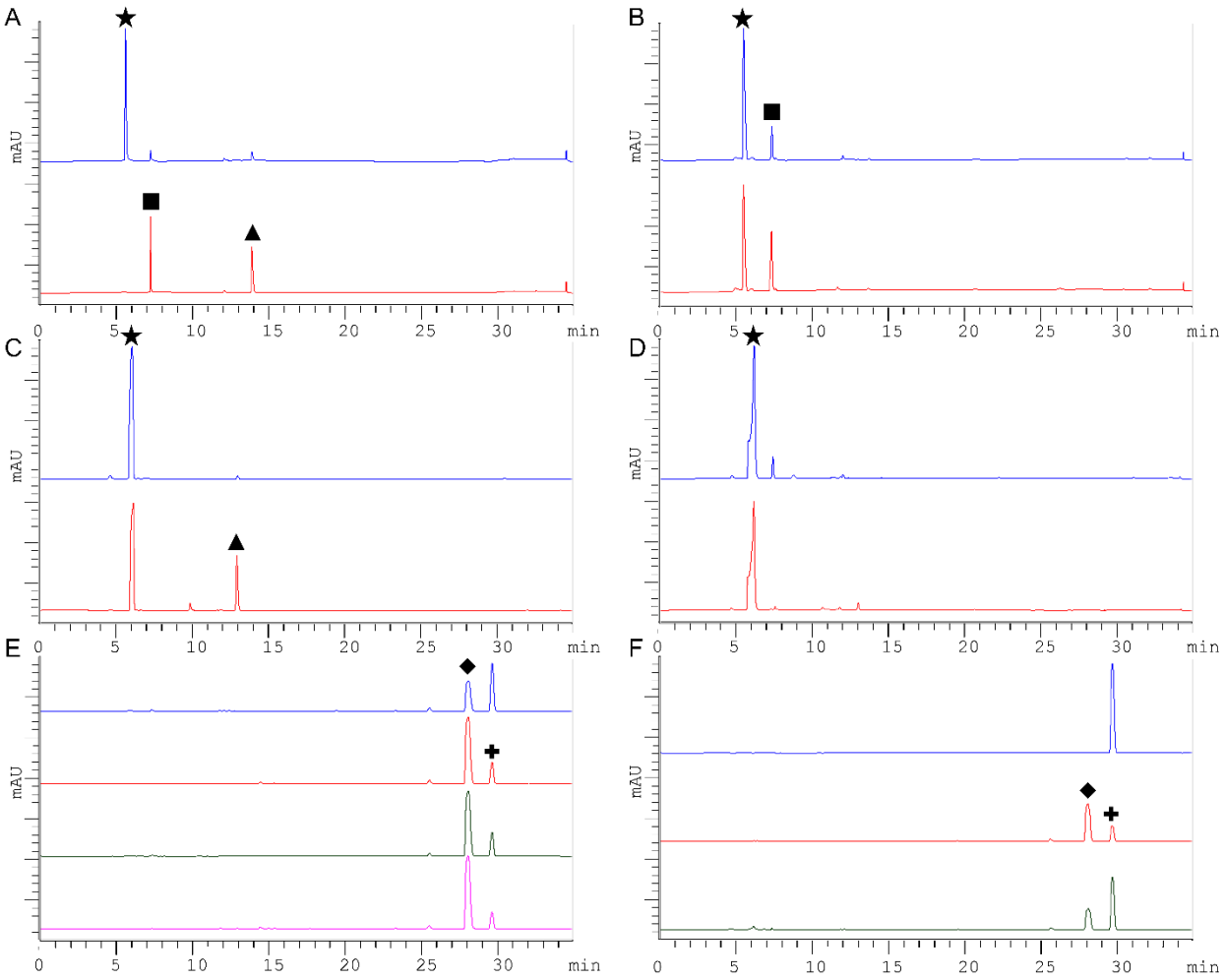

Figure S1. Representative analytical HPLC. All chromatograms were obtained using HPLC Method A. (A) AdoMet at 0 min (blue) and 1,415 min (red) (A_{260}). (B) Ado^{t}Met at 0 min (blue) and 1,450 min (red) (A_{260}). (C) ^{7dz}AdoMet at 0 min (blue) and 488 min (red) (A_{260}) where product peak broadening and UV-vis profile are consistent with commercially available starting material (^{7dz}ATP). (D) ^{7dz}Ado^{t}Met at 0 min (blue) and 1,500 min (red) (A_{260}). (E) hMAT2A-DnrK coupled reactions (10 µM hMAT2A, 30 µM DnrK, 1,000 µM ClNP) plus: L-Met (10,000 µM) and ATP (2,000 µM) (blue); L-^{t}Met (10,000 µM) and ATP (2,000 µM) (red); L-Met (10,000 µM) and ^{7dz}ATP (2,000 µM) (green); or L-^{t}Met (10,000 µM) and ^{7dz}ATP (2,000 µM) (pink) after 24 h (A_{317}). (F) 1 mM synthetic 2-chloro-1-methoxy-4-nitrobenzene standard (blue); ClNP methylation reaction (30 µM DnrK, 3,200 µM AdoMet, and 1,000 µM ClNP) after 19 h (red); co-injection of synthetic standard and ClNP methylation reaction (green) (A_{317}). AdoMet, Ado^{t}Met, ^{7dz}AdoMet, or ^{7dz}Ado^{t}Met are annotated by a star; Adenine is annotated by a square; MTA or MT^{7dz}A are annotated by a triangle; ClNP is denoted by a diamond; and 1-methoxy-2-chloro-4-nitrobenzene is annotated by a plus.

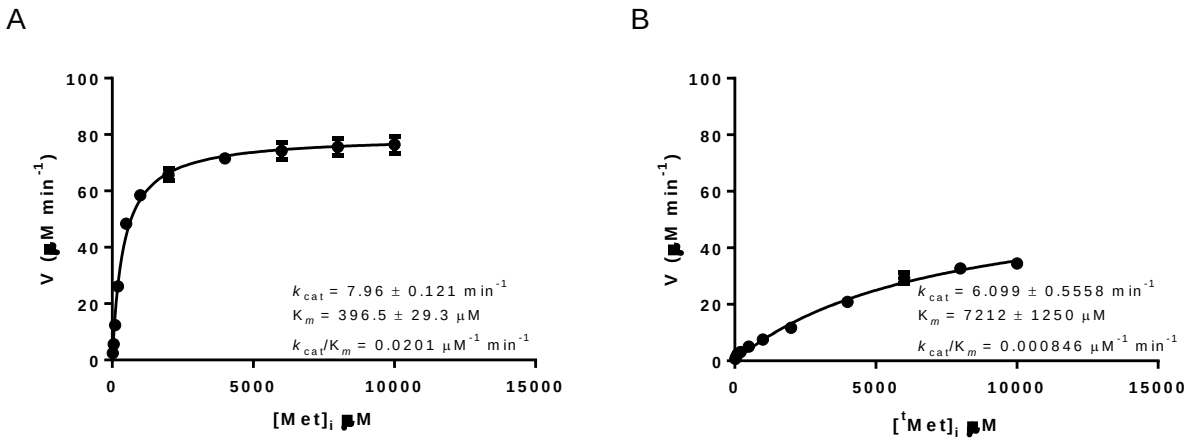

Figure S2. Determination of kinetic parameters for hMAT2A-catalyzed reactions. [hMAT2A] = 10 μM in all experiments. (A) $[ATP]_i$ = 2000 μM, $[Met]_i$ = varied. (B) $[ATP]_i$ = 2000 μM, $[^tMet]_i$ = varied.

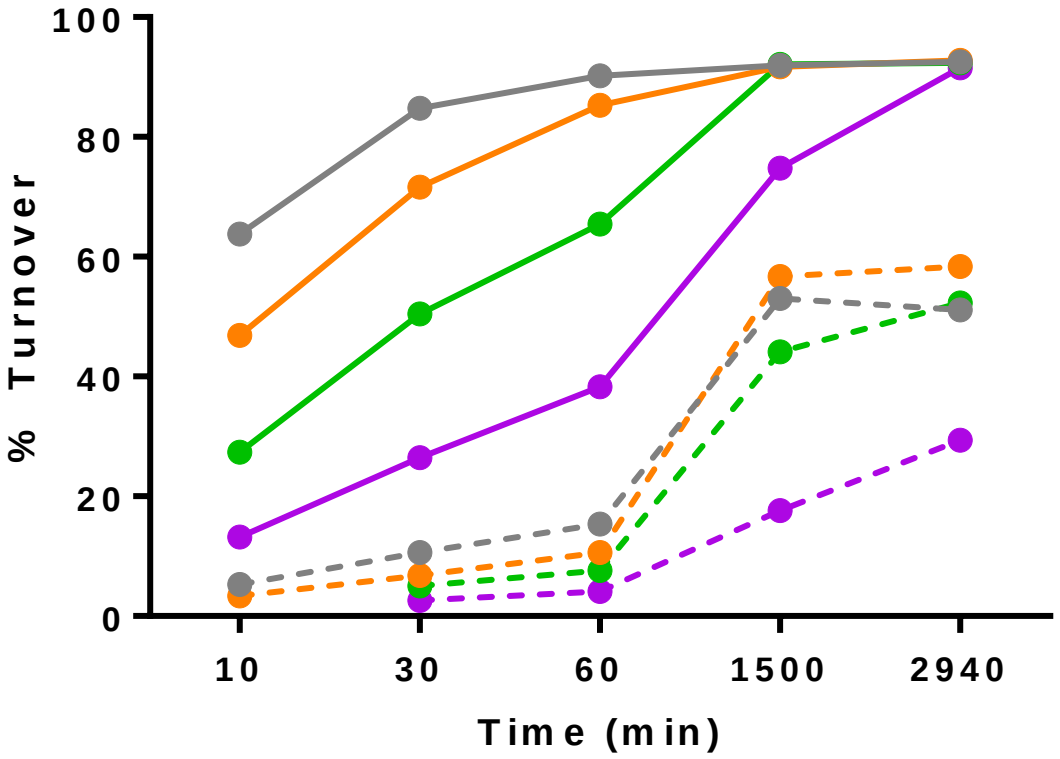

Figure S3. Turnover of ^{7dz}ATP and L-Met/**L**-^{t}Met with hMAT2A. Assay conditions are described in the Materials and Methods of the main text. $[^{7dz}ATP]_i$ = 500 µM (grey), 1,000 µM (orange), 2,000 µM(green), 4,000 µM (purple). Solid lines represent reactions with L-Met as cosubstrate, dashed with L-^{t}Met.

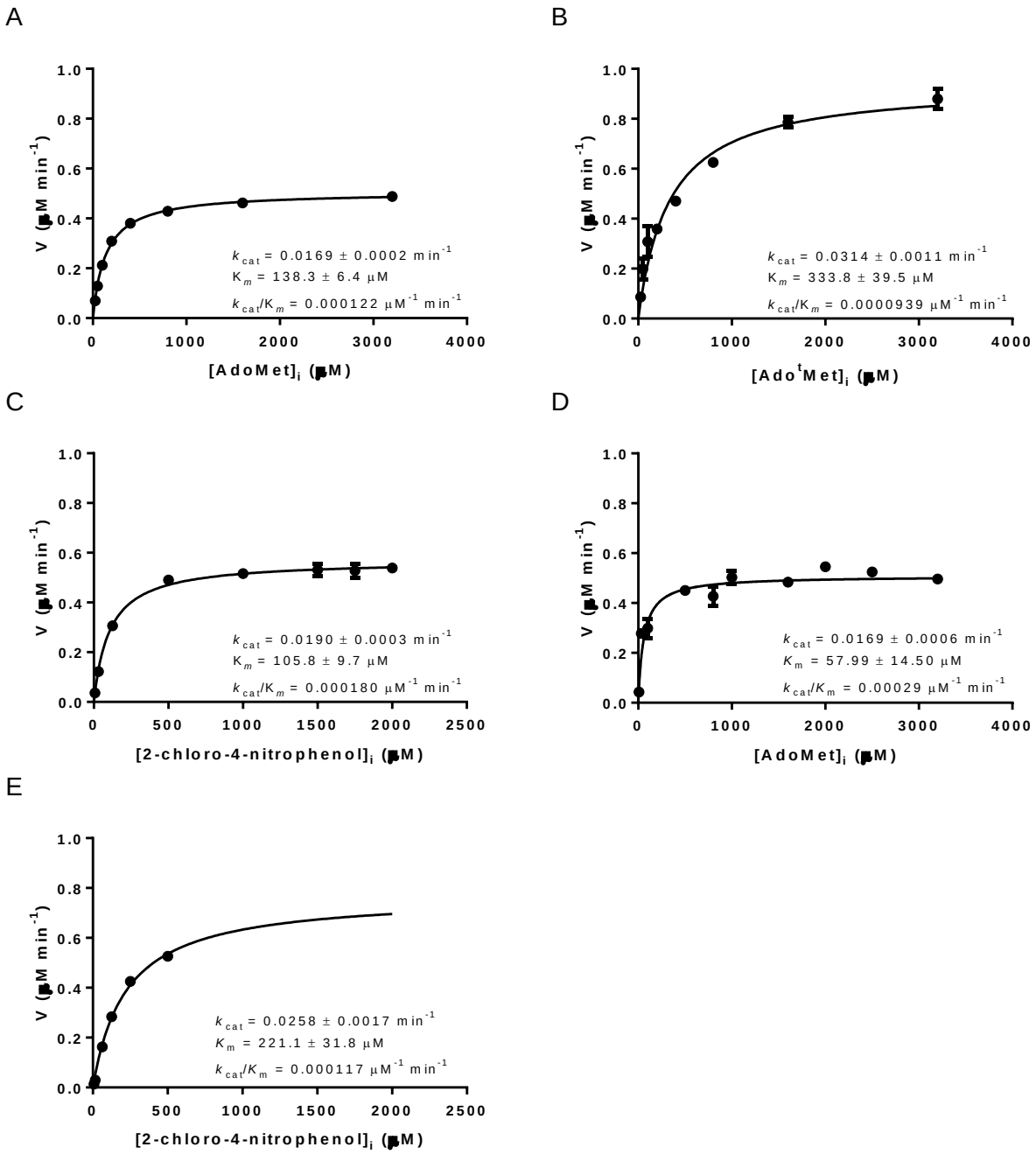

Figure S4. Determination of kinetic parameters for DnrK-catalyzed reactions. [DnrK] = 30 μM in all experiments and assays were conducted via HPLC (panels A-C) or plate-based (panels D and E) colorimetric format. (A) $[2\text{-chloro-4-nitrophenol}]_i$ = 1500 μM, $[AdoMet]_i$ = varied; (B) $[2\text{-chloro-4-nitrophenol}]_i$ = 1500 μM, $[Ado^tMet]_i$ = varied; (C) $[2\text{-chloro-4-nitrophenol}]_i$ = varied, $[AdoMet]_i$ = 1600 μM. (D) $[2\text{-chloro-4-nitrophenol}]_i$ = 500 μM, $[AdoMet]_i$ = varied; (E) $[2\text{-chloro-4-nitrophenol}]_i$ = varied, $[AdoMet]_i$ = 2,500 μM.

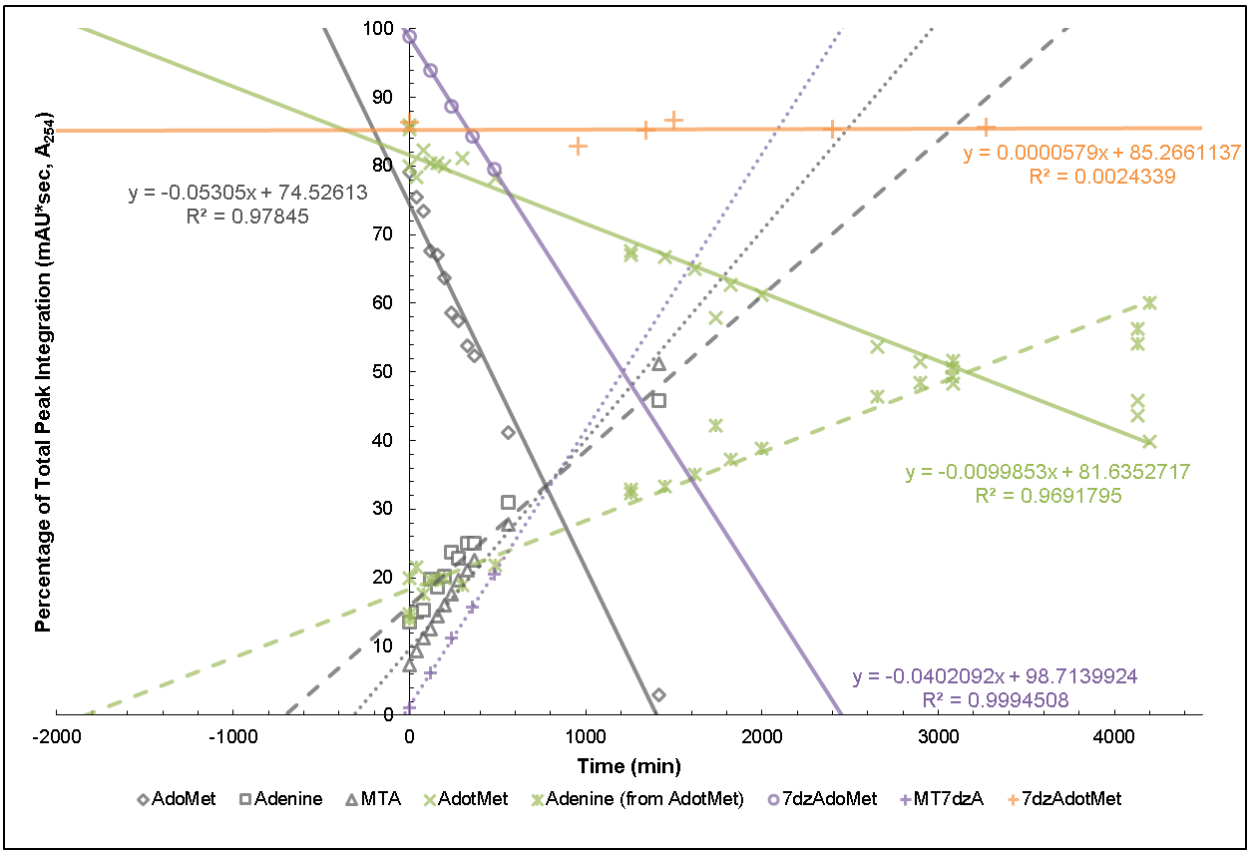

Figure S5. Time-dependent AdoMet, Ado^{t}Met, ^{7dz}AdoMet, and ^{7dz}Ado^{t}Met degradation. AdoMet (grey, solid), Ado^{t}Met (green, solid), ^{7dz}AdoMet (purple, solid), or ^{7dz}Ado^{t}Met (orange, solid) were incubated at 37 °C with 100 mM Tris·HCl, pH 8.00 and monitored via HPLC for over 55 h. Corresponding degradations products MTA (grey, dotted), MT^{7dz}A (purple, dotted), and/or adenine (grey and dashed if from AdoMet, green and dashed if from Ado^{t}Met) are also indicated.

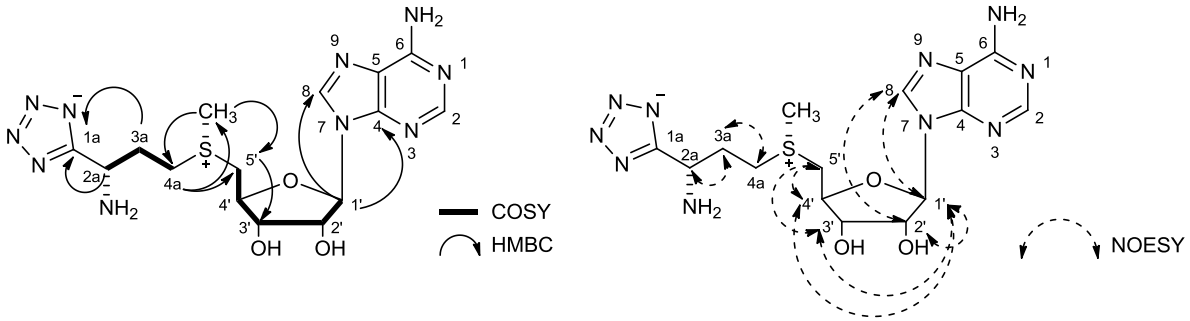

Figure S6. Key Ado^{t}Met ^{1}H–^{1}H-COSY, HMBC and NOESY correlations.

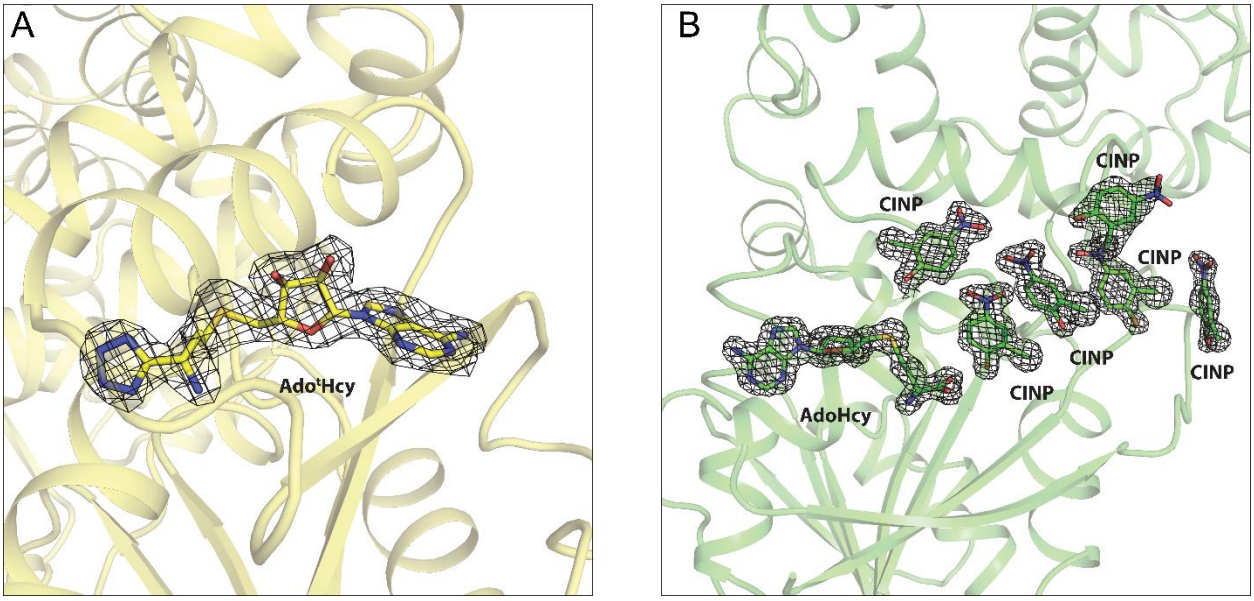

Figure S7. DnrK electron density maps. (A) *2mFo-DFc* omit map of Ado^{t}Hcy was contoured at 1.3σ. (B) *2mFo-DFc* omit map of AdoHcy and CINPs was contoured at 1.3σ.

Table S1. Turnover of ClNP in hMAT2A-DnrK coupled reactions. Assay conditions are described in the Materials and Methods of the main text.

ATP or ^{7dz}ATP	L-Met or L-^{t}Met	% Turnover
ATP	L-Met	52
ATP	L-^{t}Met	19
^{7dz}ATP	L-Met	21
^{7dz}ATP	L-^{t}Met	14

Table S2. Summary of crystal parameters, data collection, and refinement statistics. Values in parentheses are for the highest resolution shell.

	DnrK - Ado^{t}Hcy	DnrK - AdoHcy/CINPs
Crystal parameters		
Space group	*P 2$_1$*	*C 2*
Unit-cell parameters (Å, °)	60.6, 104.1, 63.0 90.0, 105.2, 90.0	123.3, 110.7, 116.9 90.0, 120.2, 90.0
Data collection statistics		
Wavelength (Å)	0.98	0.98
Resolution range (Å)	50-2.25	50-1.82
No. of reflections (measured / unique)	152,746 / 35,358	580,623 / 120,915
Completeness (%)	99.4 (96.7)	98.5 (96.5)
R_{merge}[a]	0.134 (0.346)	0.072 (0.392)
Redundancy	4.3 (4.2)	4.8 (4.3)
Mean I / sigma (I)	7.9 (3.1)	10.5 (2.8)
$CC^{1/2}$	0.99 (0.88)	0.99 (0.89)
Refinement and model statistics		
R_{cryst} / R_{free}	0.184 / 0.246	0.154 / 0.186
Ligands RSCC[b]	0.98	0.95
RMSD bonds (Å)	0.011	0.007
RMSD angles (°)	1.31	1.12
B factor - protein/ligand/solvent (Å^2)	23.1 / 13.5 / 31.4	31.1 / 29.9 / 41.6
No. of protein atoms	5,137	8,138
No. of waters	491	913
No. of auxiliary molecules in 1 chain	1 Ado^{t}Hcy	1 AdoHcy, 6 CINPs
Ramachandran plot (%)		
Favorable region	98.0	98.2
Additional allowed region	2.0	1.8
Disallowed region	0.0	0.0
PDB	5EEG	5EEH

[a] $R_{merge} = \sum_h \sum_i | I_i(h) - \langle I(h) \rangle | / \sum_h \sum_i I_i(h)$, where $I_i(h)$ is the intensity of an individual measurement of the reflection and $\langle I(h) \rangle$ is the mean intensity of the reflection.
[b] ligand RSCC is ligand real-space correlation coefficient, which provides an objective measure of the fit of atom coordinates to electron density.